**Proceedings of the**
**International Conference on Mechanical Engineering 2011**
**(ICME2011) 18-20 December 2011, Dhaka, Bangladesh**

**ICME2011-KEY-004**

# HOMOGENEOUS NUCLEATION BOILING EXPLOSION PHENOMENA UNDER NON-EQUILIBRIUM CONDITION

**Masanori Monde and Mohammad Nasim Hasan**

Department of Mechanical Engineering, Saga University, Japan

## ABSTRACT

A new theoretical model has been developed to study homogeneous boiling explosion phenomena under non-equilibrium liquid heating condition. In this model, a finite liquid control volume or cluster having the size of a characteristic critical embryo at the liquid boundary has been considered and the corresponding energy balance equation is obtained by considering two parallel competing processes taking place inside the liquid cluster, namely, transient energy deposition and internal energy consumption due to a bubble nucleation and its growth. Depending on the instantaneous rate of external energy deposition and boiling heat consumption within the liquid cluster, a particular state has been defined as the condition of boiling explosion i.e. the onset of mass scale vaporization in which the bubble generation and its growth cause the liquid sensible energy to decrease. The obtained results have been presented in terms of the average temperature rise within the liquid cluster, maximum attainable liquid temperature prior to the boiling explosion and the time required achieving the condition of the boiling explosion for three different liquid heating cases, namely (i) linearly increasing temperature condition, (ii) high heat flux pulse heating condition and (iii) constant boundary temperature condition. With the initial and boundary conditions identical to those reported in literature, model results have been found to be in good agreement with the experimental observations for all of these liquid heating cases. The boiling explosion condition as predicted by the developed model has been verified by comparing the heat flux across the liquid–vapor interface at the boiling explosion with the corresponding limit of maximum possible heat flux, $q_{max,max}$. Moreover, the limiting condition for the occurrence of homogeneous boiling explosion in water at atmospheric pressure has been determined by applying the present model for any liquid heating condition.

**Keywords:** Boiling Explosion, Homogeneous Nucleation Boiling, Linear Liquid Boundary Heating, High Heat Flux Pulse Heating, Liquid Contact with High Temperature Surface, Lower Limit of Homogeneous Nucleation Boiling.

## 1. INTRODUCTION

In classical thermodynamics, phase transitions like boiling for simple compressible substances are treated as quasi-equilibrium events at conditions corresponding to the saturation state. However, in real phase change phenomena a deviation from classical thermodynamics occurs under non-equilibrium condition such as a liquid superheating above the boiling point during vaporization. Liquid superheating might be obtained either by heating it rapidly at constant pressure or by depressurizing it rapidly at constant temperature. In either case, the liquid penetrates into a region of non-equilibrium state or metastable state in which the liquid temperature becomes higher than the saturation temperature at the prevailing pressure. The degree of such liquid superheating often ranges from a few tenths of a degree to several tens of degrees, depending on, for example the liquid, the nature of liquid container, the volume of liquid, the purity of liquid and the rate of parametric variation, i.e., liquid heating rate or depressurization rate. In the limiting case of no vapor contact which can be idealized for extremely fast parametric change it is possible to achieve remarkably high degrees of superheat at which boiling is initiated mainly by homogeneous nucleation of bubbles which is followed immediately by a large scale boiling–usually with explosive force. This instantaneous abrupt phase change phenomenon is technically referred to as boiling explosion or explosive boiling. This kind of boiling explosion resulting from liquid superheating is omnipresent in many industrial as well as natural phenomena. In several industrial processes such as in paper [1], cryogenic [2], and metal processing industries [3], two liquids having different temperatures often come in contact. If the hotter liquid is relatively non-volatile (smelt, molten metal etc.) and the colder liquid is relatively volatile (water, refrigerant etc.), the later can be superheated to a point where it vaporizes rapidly in a massive scale that can cause injury to personnel as well as considerable structural damage [4]. The sudden depressurization of a liquefied gas either intentionally

(through the operation of a pressure relief valve) or accidentally (through a loss of containment) can lead to disastrous consequences called BLEVE (Boiling Liquid Expanding Vapor Explosion) accident [5, 6]. In the nuclear power industry, overheating of a reactor's core might cause the fuel rod to melt (hot, nonvolatile liquid) and subsequently to interact with the coolant (cold, volatile liquid) thereby leading to the well known molten fuel-coolant interaction [7]. In fact the disastrous accidents caused by the explosive boiling in various applications motivated the early researches on explosive boiling concerned to safety premise. It also occurs when a liquid comes in contact with a hot surface as in case of jet impingent quenching [8, 9]. While uncontrolled boiling explosion poses a potential hazard, boiling explosion when it is produced in a controlled manner it has many interesting and practical applications ranging from ink jet printer [10] to microelectronic cooling devices and micro bubble actuators in MEMS devices [11]. Boiling explosion following rapid liquid heating has also been applied successfully in laser cleaning, laser surgery, design and thermal control of space shuttles. Researches are underway in the technical development of bubble-actuated micro-fluidic devices, such as drug delivery systems [12], vapor bubble micro pumps [13], micro injectors [14], micro thrusters and thermal bubble perturbators [15]. Due to very small space and time scale, some abnormal phenomena occur in these thermal micromachines and MEMS applications that no longer fit with the classical heat transfer theory. The associated boiling phenomena differ from usual nucleate boiling in many aspects. First, the bubble nucleation is initiated at a higher temperature close to the theoretical superheat limit. Second, the boiling process is much explosive because the initial bubble pressure is very high. Third, the boiling process is more reproducible because its mechanism is mainly governed by the property of the liquid (i.e. homogeneous nucleation) rather than by the surface characteristics (i.e. heterogeneous nucleation). Successful extraction of the work from high pressure rapidly expanding vapor bubbles generated by microscopic boiling/vapor explosion could revolutionize the design and performance of these abovementioned thermal micromachines. Therefore, micro scale boiling explosion phenomena has been one of the hot frontier topics in the research of heat transfer and considerable effort has been devoted to a better understanding of the fundamental science and mechanism of boiling explosion phenomena.

### 1.1 Homogeneous Nucleation Boiling Explosion–From Equilibrium Viewpoint

The superheat limit of a liquid i.e. the maximum attainable temperature to which a liquid can be heated before it vaporizes spontaneously can be determined theoretically in two different approaches. One approach is based on the mechanical stability consideration of classical thermodynamics and the superheat limit is known as the thermodynamic superheat limit or the spinodal limit, $T_{TSL}$, which indeed represents the deepest possible penetration of liquid in the domain of metastable states. At constant pressure and composition, this limit is the locus of the minima in the liquid isotherms, i.e. the spinodal curve of the liquid which satisfies the conditions $(\partial P/\partial V)_T = 0$ and $(\partial^2 P/\partial V^2)_T > 0$. This spinodal curves separates the metastable region which satisfies the mechanical stability condition, $(\partial P/\partial V)_T < 0$, from the unstable region $(\partial P/\partial V)_T > 0$. In the stable and metastable regions, local density fluctuations damp out with time and therefore the liquid and vapor may remain in its form indefinitely, whereas in the unstable region, even the smallest fluctuation grows up. A typical liquid spinodal curve is illustrated in Fig. 1 as the line C–C´–Critical point. The shaded area between the liquid spinodal and the two phase boundary (the line B–Critical point) represents the metastable superheated fluid. The calculated value of the spinodal generally depends upon the equation of state used for the analysis [16]. For instance, using the Van der Waals equation of state, Spiegler et al. [17] derived the condition of mechanical stability i.e. the thermodynamic superheat limit, $T_{TSL}$, as

$$T_{TSL} = 0.844 T_c \quad (1)$$

For fluids at higher pressures up to the critical point, Lienhard [18] proposed the following correlation for the thermodynamic superheat limit, $T_{TSL}$.

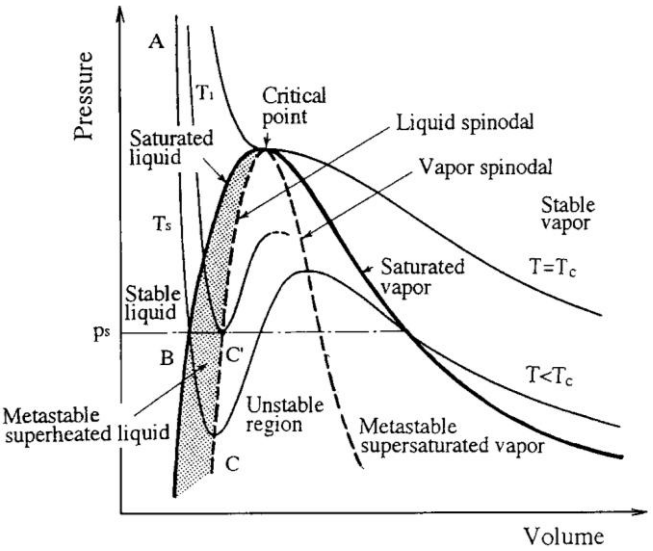


Fig 1. Pressure– volume chart of fluid and the range of metastable superheated liquid [19].

$$\frac{(T_{TSL} - T_s)}{T_c} = 0.905 \left(\frac{T_s}{T_c}\right) + 0.095 \left(\frac{T_s}{T_c}\right)^8 \quad (2)$$

where $T_c$ is the critical temperature (K) and $T_s$ is the saturation temperature (K), respectively.

The second approach to describe the maximum liquid superheat temperature is referred to as the kinetic homogeneous nucleation theory [20–22] which bases the temperature and pressure dependence of bubble nucleation on molecular fluctuation probability. At and above saturation condition, molecular fluctuation occurs in such a way to cause a localized decrease in the liquid density, leading to the formation of vapor embryos. The fluctuation probability increases with temperature and at

the superheat limit the probability of a high bubble embryo formation rate i.e. a threshold nucleation rate is sufficient to transform the liquid to vapor. This superheat limit is often termed as the homogeneous nucleation temperature or the spontaneous nucleation temperature. According to the classical homogeneous nucleation theory, for a liquid at temperature, $T_l$, the largest nucleation rate, $J$, per unit liquid volume can be given as [22–23]

$$J(T_l) = N_l f \exp\left(\frac{W_{min}}{k_B T_l}\right) \quad (3)$$

In Eq. (3), $N_l$ denotes the number density of liquid molecules, $f$ represents the frequency factor and $k_B$ denotes the Boltzmann constant while $W_{min}$ denotes the free energy of formation of a critical nucleus. Equation (3) is the general form of homogeneous nucleation rate equation. On further simplification, Carey [23] obtained:

$$J(T_l) = N_l \sqrt{\frac{3\sigma}{\pi m}} \exp\left(\frac{16\pi\sigma^3}{3k_B T_l \{P_s(T_l) - P_0\}^2}\right) \quad (4)$$

where $\sigma$, $m$, $P_0$ and $P_s$ denote the liquid surface tension, the molecular mass of the liquid, the bulk liquid pressure and the saturation pressure respectively. Equation (4) can be solved iteratively to determine the kinetic limit of superheat, if a threshold value of $J$ corresponding to the onset of homogeneous nucleation is assumed. From experimental superheat data for a large variety of fluids at atmospheric pressure, Blander and Katz [22] obtained a threshold value of $10^{12}$ nuclei/($m^3$s). As mentioned by Cole [23], a threshold nucleation rate of $10^6$ nuclei/($m^3$s) gives perfectly acceptable results for the limiting kinetic superheat temperature in most situations. Carey [24] also proposed a value of $10^{12}$ nuclei/($m^3$s) as the threshold nucleation rate.

### 1.2 Homogeneous Nucleation Boiling Explosion–In Experiments

In the laboratory, microscale boiling explosion has been generated and studied usually by heating liquids with thin wires, thin-film microheaters, and high energy laser beams. Fine platinum wire/planar heaters subjected to ramp heating have been extensively used for transient boiling study in earlier works where the temperature of the wire was determined by the principle of resistance thermometry. Recent advancement in MEMS technology has also enabled the fabrication of polysilicon film microheaters with its surface totally free from noticeable cavities in micron or even submicron scale that resulted in much high heat flux from the heater surface. A number of researchers have also focused on the microscale boiling explosion phenomena occurring upon liquid contact with preheated solid surface or during mixing with non-volatile hot liquids. A review of earlier research works on explosive boiling by using various liquid heating techniques has been made in the next.

#### 1.2.1 Liquid Heating with a Linearly Increasing Temperature

Skripov [25] discussed explosive boiling phenomena of liquids under rapid heating for two typical processes: bulk heating and boundary/surface heating. The first process corresponds to the process of liquid heating by intense infrared or laser radiation while the second process refers to rapid heating of dissolved electrolytes or immersed metal wire by an electric current. They performed transient boiling experiments on a fine wire under rapid heating in organic liquids and demonstrated that it is possible to superheat the liquid to its homogeneous nucleation temperature, where the molecular energy fluctuations become the dominant mechanism for vapor generation. The condition of explosive boiling named as the impact boiling condition were defined as the minimum heating rate necessary to induce in the liquid to the kinetic limit of liquid superheat. Their experiments [26] showed that a heating rate of greater than $6.0\times10^6$ K/s was required for homogenous nucleation around a platinum heating wire immersed in water at atmospheric pressure. Derewnicki [27] studied transient boiling in water using a thin platinum wire of 25 μm in diameter under slow and rapid heating at various system pressures. At a slow heating rate of about $9.0\times10^5$ K/s, before taking place the nucleation, the temporal temperature variation of the platinum wire was found to follow the theoretical solution for transient heat conduction and to be independent of system pressure. At atmospheric pressure, the bubble nucleation temperature was noted to be about 200 °C and only few active heterogeneous nucleation sites were found. On the other hand, at a heating rate of about $6.0\times10^6$ K/s, the bubble nucleation temperature was obtained to be around 300 °C that was found to be relatively independent of the system pressure. Gold et al. [28] also investigated the explosive vaporization in water from a platinum wire of 10 μm in diameter and 1 mm in length. At a slow heating rate of $10^5$ K/s, the nucleation was found to be initiated by a single vapor bubble growing from a cavity on the wire surface which subsequently triggered the boiling on the entire wire surface with the heterogeneous nucleation being the main mechanism. It was found that the nucleation temperature increased with the heating rate until a maximum limit is reached. At the maximum heating rate of $86.0\times10^6$ K/s, the wire surface was almost instantaneously covered with a thin vapor film. A maximum nucleation temperature of 303 °C was obtained at the maximum heating rate of $86.0\times10^6$ K/s when homogeneous nucleation occurred. Iida et al. [29–30] experimentally observed the boiling nucleation phenomenon in various liquids (ethyl alcohol, toluene and water) occurring at high boundary heating rates of up to $9.3\times10^7$ K/s using a small platinum film heater (effective heating area of 100 × 400 μm) that allows simultaneous precise measurement of heater temperature. The heater temperature at the boiling incipience was saturated at approximately $1.0\times10^7$ K/s for ethyl alcohol and toluene (at approximately $4.5\times10^7$ K/s for water) and for ethyl alcohol, this value agreed well with the homogeneous nucleation temperature. They found a number of tiny bubbles at uniform size to generate immediately after the boiling incipience and the number of bubbles tended to increase as predicted by the homogeneous nucleation theory. From the observed phenomena, they concluded that bubble generation

during rapid liquid heating is due primarily to spontaneous nucleation or homogeneous nucleation. Okuyama et al. [31] investigated the dynamics of boiling process and the spontaneous nucleation on a small film heater immersed in water and ethyl alcohol for even much boundary heating rates ranging from $10^7$ K/s to approximately $10^9$ K/s. Under these extreme liquid heating conditions, they found the spontaneous nucleation to be dominant for the inception of boiling. Immediately after the concurrent generation of a large number of fine bubbles, a vapor film was formed by the coalescence that rapidly expanded to a single bubble. With the increase of the heating rate, the coalesced bubble was found to flatten and only a thin vapor film was noticed to grow before cavitation collapse. Avedisian et al. [32] measured the average temperature of a Ta/Al heater on a silicon substrate which was immersed in subcooled water during pulse heating at microsecond duration. It was found that the bubble nucleation temperature increased with the heating rate and approached a maximum value of 270 °C, corresponding to a maximum heating rate of $2.5 \times 10^8$ K/s. Furthermore, the measured nucleation temperature was found in qualitative agreement with the prediction of homogeneous boiling theory for an appropriate value of the contact angle. Kuznetsov and Kozulin [33] experimentally studied the explosive vaporization of a water layer during a temperature rising rate up to about $1.80 \times 10^8$ K/s using a microheater ($100 \times 100$ μm) coated with a silicon-carbide layer and recorded the time history of the vaporization process and the dynamics of the steam blanket generated on the heater surface. The observed temperature at the beginning of explosive vaporization over the silicon carbide surface was found to be lower than the spinodal temperature.

### 1.2.2 Liquid Heating With A High Heat Flux

Asai et al. [34–36] conducted a series of theoretical and experimental studies on bubble nucleation and growth in water-based ink and methyl alcohol under typical operating condition of thermal ink jet printer. A one dimensional numerical model of bubble growth and collapse and the resulting flow motion on a typical bubble jet printing head (effective heating area $150 \times 30$ μm) was presented by Asai [34]. Later, Asai [35] presented another theoretical model to predict the nucleation process in water based ink. In his model, nucleation probability was derived and used to simulate the initial bubble growth process. Model prediction was confirmed by experimentations conducted with a prototype bubble jet printing head (effective heating area $150 \times 30$ μm) for heat fluxes ranging from 100 MW/m$^2$ to 200 MW/m$^2$. In this study, the incipient boiling time was pointed out as a stochastic variable rather a point value which became more reproducible as the heat input was increased. Asai [35] mentioned about a sufficiently large heat flux (~ 100 MW/m$^2$) and threshold heat pulse duration for powerful reproducible bubble formation. Asai [36] also described another model of bubble dynamics under high heat flux pulse heating conditions. The proposed model was validated by experimentation using a thin film heater ($100 \times 100$ μm) for methanol heating with high heat fluxes from 5 to 50 MW/m$^2$. From agreement between experimental result and theoretical prediction, they implied that the dominant bubble generation mechanism was the spontaneous nucleation of liquids due to thermal fluctuation i.e. the homogeneous nucleation.

Yin et al. [37] studied the bubble nucleation process in FC-72 on an impulsively powered square microheater ($260 \times 260$ μm) for pulse widths of 1–10 ms duration at different heat fluxes between 3 and 44 MW/m$^2$. At a low heat flux of 3.43 MW/m$^2$, a single large bubble consistently appeared near the center of the heater that grew very dynamically overshooting its equilibrium size, shrinked and then essentially stabilized over the heater while at high heat flux of 44 MW/m$^2$, nucleation occurred at several spots on the heater. Varlamov et al. [38] experimentally observed explosive boiling of liquids (water, toluene, ethanol, and isopropyl alcohol) on film heaters under the action of pulsed heat fluxes of 100–1000 MW/m$^2$ by using stroboscopic visualization technique with a time resolution of 100 nsec. From their observation, they figured out the specific conditions of thermal effect (magnitude of heat flux, duration and repetition frequency of the heat pulse) which ensure single and repeated boiling, intermittent boiling, and boiling with formation of complicated multi-bubble structures. From the experimental data and their comparison with theoretical prediction, they concluded that homogeneous nucleation was the dominant mechanism for boiling in all liquids under consideration for heat fluxes higher than 100 MW/m$^2$.

Hong et al. [39] carried out experimental study of the rapid formation and collapse of bubbles formed on a microheater ($25 \times 80$ μm) induced by pulse heating. In this study, a high heat flux pulses of more than 750 MW/m$^2$ was applied to the resistive heater with the pulse heating duration being varied from 1 to 4 μs. From experimental observation, they mentioned a threshold pulse duration above which the maximum size of the bubble does not change anymore. However, the maximum bubble size was found to increase with an increase in the liquid initial temperature. They obtained the nucleation temperature for water slightly below the theoretical superheat limit and found a weak linear dependency on the heating rate. They mentioned the mechanism of the bubble formation to be a combined homogeneous-heterogeneous nucleation.

Xu and Zhang [40] studied the effect of pulse heating parameters on the micro bubble behavior of a platinum microheater ($100 \times 20$ μm) immersed in a methanol pool with heat fluxes of 10–37 MW/m$^2$ and pulse frequency of 25–500 Hz. The boiling incipience temperature was found as the superheat limit of methanol, corresponding to the homogeneous nucleation.

### 1.2.3 Liquid heating during contact with hot liquid/solid

The boiling explosion phenomena occuring in liquid-liquid system is often known as the vapor explosion. Henry and Fauske [41] identified the necessary conditions for the occurrence of the boiling explosion phenomena in liquid-liquid systems such as (i)

the threshold temperature for spontaneous nucleation in the cold liquid, (ii) the existence of stable film boiling to sustain vapor embryos of the critical size prior to boiling explosion, (iii) the size of cold liquid drops exceeding a critical value to be captured by the hot liquid surface, and (iv) the interfacial temperature between the two liquids exceeding the homogeneous nucleation temperature. Ochiai and Bankoff [42] proposed the 'splash' theory, which states that splash (instantaneous boiling or vapor explosion) occurs within the temperature range, $T_{sn} < T_i < T_c$ where $T_{sn}$ and $T_c$ denote the spontaneous nucleation temperature and the critical temperature of the cold liquid while $T_i$ denotes the interfacial temperature between the two liquids.

Iida et al. [43] conducted experiments on vapor explosion resulting from mixing of a molten salt drop such as LiCl or $LiNO_3$ in water. They observed that stable film boiling and $T_i > T_{sn}$ were necessary condition for vapor explosion in the molten salt-liquid system. They also mentioned that both the hot and cold liquids had the upper and lower temperature limits for vapor explosion. Investigations of the boiling explosion phenomena using high energy laser irradiation have also been carried out by some researchers that include Ueno et al. [44], Huai et al. [45, 46] and Geints et al. [47]. These investigations also manifested the effect of liquid heating intensity on the nature and limit of bubble nucleation.

While researches on boiling explosion by using ultra thin heating wire, thin film microheater and high energy laser beam, focused on the mechanism of boiling nucleation and growth, the potential of exploding vapor to perform work on the surrounding bulk liquid etc., research on the boiling phenomena upon liquid contact with a hot surface has been found to pose a significantly different issue that is when liquid can wet a hot surface. In the simplest case of pool boiling, the initial dry state refers to film boiling while the wet state corresponds to the nucleate boiling. Therefore, the limiting condition under consideration has been described as the minimum film boiling (MFB) temperature, minimum heat flux (MHF) temperature or the temperature of film boiling destabilization by some scientists. Some other scientists also addressed the similar phenomena with other synonyms that include the rewetting temperature, the Leidenfrost temperature etc. However, the Leidenfrost temperature still remains a poor understood phenomenon in context of solid-liquid contact heat transfer.

Spiegler et al. [17] described the rewetting temperature in terms of the maximum superheat temperature of the liquid because above this temperature the liquid would immediately boil explosively and thus could not touch the surface. Rewetting model based on this maximum superheat temperature hypothesis, usually consider that the rewetting will not occur at the liquid temperature at the contact point that is the interface between the solid and the liquid is higher than the maximum temperature the liquid can exist. For instance, Spiegler et al. [17] considered the maximum superheat limit as the spinodal limit obtained for the Van der Waals equation of state for the liquid as shown in Eq. (1), while the interfacial liquid temperature has been approximated by infinite slab model which considers that both the solid and liquid behave like two semi-infinite slabs of uniform initial temperatures that are suddenly brought into contact.

Gunnerson and Cronenberg [48] proposed a thermodynamic model for the prediction of the temperature for film boiling destabilization and discussed its relation with vapor explosion phenomena. In their model, they also considered the solid-liquid contact phenomena as a two 1-D semi-infinite body contact problem as done by Spiegler et al. [17]. For a perfectly smooth surface, they considered the boiling to occur at an interfacial temperature being equal to the maximum liquid superheat while for imperfect interface, they assumed the boiling to occur at a minimum interfacial temperature being equal to the liquid saturation temperature at the prevailing pressure. Considering the Leidenfrost temperature as the minimum wall temperature for film boiling, they proposed a range of theoretical Leidenfrost temperature that is the wall temperatures at these two extreme situations for a particular solid-liquid combination.

Gerweck and Yadigaroglu [49] studied the liquid to vapor transition process that occurs when the liquid comes in to contact with a hot wall. They used statistical mechanics to derive an approximate local equation of state for the fluid as a function of distance from the wall. They arrived at a wall rewetting condition different from the minimum film temperature. They defined the rewetting temperature as the temperature at which the liquid can touch the wall without being immediately turned into vapor. The immediate phase change denoted herein referred to the explosive vaporization of the liquid near the maximum liquid superheat. They concluded that the spinodal temperature be a good estimation for the maximum superheat temperature that a liquid can sustain on a wall for most situations encountered in rewetting experiments.

Inada and Yang [50] experimentally observed the boiling phenomena of single water drops upon impingement on a heated surface. Vapor micro-explosions were captured by a high speed video camera. Measurements were made on the frequency and amplitude of the elastic longitudinal waves produced by boiling and the acoustic pressure of boiling sound by using a piezo-electric potential transformer and a condenser microphone, respectively. They found the maximum frequency and amplitude of the elastic-longitudinal waves and the maximum values of the boiling acoustic pressure to occur in a certain range of the surface temperatures for violent miniaturization of sessile drops. Moreover, the range of the surface temperatures coincided with that of the transition boiling regime around the homogeneous nucleation temperature of the liquid. They described the miniaturization phenomena to be induced by an explosive boiling resulting from a direct contact between parts of the liquid and the heating surface.

Woodfield et al. [8] used a high-speed video camera and microphone to capture the flow behavior and boiling sound of a free-surface water jet impinging on a high temperature surface during quench cooling. Depending

on the superheat of the surface, Woodfiled et al. [8] obtained considerably different flow patterns. For the cases where the initial surface temperature was above about 300 °C an almost explosive pattern appeared which was in contrast to slightly lower temperatures where a liquid sheet flow structure was apparent. The change in flow phenomena was accompanied by a sudden change in the boiling sound and an increase in the heat transfer rate. Islam et al. [9] also mentioned that the occurrence of boiling explosion due to homogeneous and/or heterogeneous nucleation boiling hinders the establishment of the stable solid-liquid contact during jet impingement quenching. Their observation also revealed out that a stable solid-liquid contact during jet impingement quenching occurs when the surface temperature is cooled down below a certain limit when no boiling explosion occurs as indicated by a visible "wet patch" on the hot surface beneath the impinging jet.

### 1.2.4 Motivation behind the Present Work

Most of the previous studies on explosive boiling following rapid liquid heating have focused on the incipience condition of bubble generation, the mechanism of boiling nucleation, and the effect of rapid oscillation of bubble growth and collapse on liquid motion and the heater involved. The condition of boiling incipience and that of boiling explosion are quite different and which condition corresponds to the boiling explosion remains unclear. A clear understanding of the boiling explosion condition is necessary in order to better predict the frequency of boiling-actuated devices and to improve micro-heater design. For various practical reasons, ascertaining the boiling explosion condition experimentally for different heating conditions is difficult and sometimes almost impossible especially at extremely high rates of liquid heating. The theoretical model described by Elias and Chambre´ [51] seems inadequate to handle the process of transient non-uniform liquid heating as it does not take any account of the liquid thickness enough for the boiling explosion to take place. So it is important to develop new model by taking account of an appropriate liquid volume for the treatment of realistic transient non-uniform liquid heating cases. In the present paper, a new theoretical model has been developed for the process of rapid, non-uniform transient liquid heating and subsequent boiling explosion. Based on the instantaneous energy consumption rate of bubble generation and growth by homogeneous nucleation, a particular state of liquid heating has been defined as the boiling explosion condition in this model. The model developed in the present study [52] will be briefly explained and summarized in the next chapter.

## 2. NEW MODEL FOR BOILING EXPLOSION

First, a liquid control volume or cluster is focused on the liquid-solid interface as shown in Fig. 2 where heat has been stored by conduction, while some of the stored heat in the cluster will be consumed to generate bubbles. The cluster size is much smaller than a macroscopic observed event so that what takes place around the cluster may be assumed to be treated with as one dimensional heat conduction in semi-infinite stagnant liquid. As the liquid temperature field is transient and non-uniform, determination of the cluster size becomes very important. For instance, Carey [24] proposed the following equation for the radius of equilibrium critical vapor embryo ($r_c$) in a superheated liquid ($T_l$) as

$$r_c = \frac{2\sigma(T_l)}{P_s(T_l)\exp\left[\left\{P_o - P_s(T_l)\right\}/\rho_l R T_l\right] - P_o} \qquad (5)$$

Equation (5) gives a critical condition that the embryo will spontaneously grow or not depending on whether it becomes larger than the size of $r = r_c$ or not with an energetic point of view against a meta-stable bubbles. The variation of the radius of critical vapor embryo, $r_c$, with the liquid temperature, $T_l$, can be calculated by Eq. (5) and is shown in Fig. 3. As depicted in Fig. 3, $r_c$ decreases gradually with increasing liquid temperature.

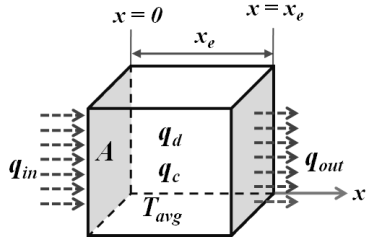


Fig. 2: Schematic of the liquid control volume/cluster

In this model, we adopt this embryo size ($2r_c$) at maximum liquid superheat ($T^*_{avg}$) as the cluster size ($x_e$) i.e., $x_e = 2r_c$ in the liquid. The net increase in the internal energy of the liquid cluster depends on transient energy deposition as well as transient energy consumption due to bubble nucleation and growth which can be obtained in terms of the average temperature in the liquid cluster as follows:

$$\frac{dT_{avg}}{dt} = \frac{d}{dt}\left[\frac{1}{x_e}\int_0^{x_e} T(x,t)dx\right] = \frac{1}{\rho_l c_l x_e}\left[q_d(t) - q_c(t)\right] \qquad (6)$$

This model defines whether the homogeneous nucleation boiling explosion takes place or not, depends on whether $dT_{avg}/dt < 0$ or not. In other words, if, $dT_{avg}/dt > 0$, then the heat still continues to be stored, while, if, $dT_{avg}/dt < 0$, then the necessary heat consumption for the generation and growth of the bubbles, becomes at a moment larger than the amount of external heat supply. The huge amount of heat consumption would bring the liquid superheat into a catastrophic vaporization, namely, a state called boiling or vapor explosion. The corresponding time at the onset of the condition, $dT_{avg}/dt = 0$, with the attainable limit of cluster temperatureis denoted by $t^*$, as the time of homogeneous boiling explosion.

The rate of energy deposition in the cluster, $q_d(t)$, due to heat conduction can be obtained from the difference in heat fluxes across the cluster as

$$q_d(t) = -\lambda_l \left\{ \left.\frac{\partial T}{\partial x}\right|_{x=0} - \left.\frac{\partial T}{\partial x}\right|_{x=x_e} \right\} \qquad (7)$$

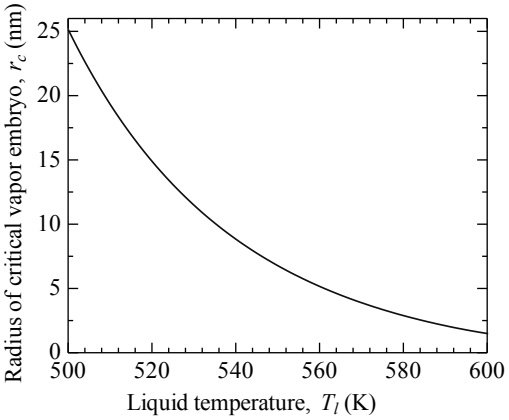


Fig 3. Radius of critical vapor embryo ($r_c$) at various liquid temperatures for water at atmospheric pressure.

In order to calculate the heat fluxes on both sides of the liquid cluster as in Eq. (7), we need a boundary condition for the cluster, for which one-dimensional heat conduction can be solved. We may focus three different boundary conditions such as linearly increasing temperature condition [28–31] or constant temperature condition like jet impingement quenching [8, 9] or a constant high heat flux heating condition [34–36, 38, 39].

The rate of energy consumption, $q_c(t)$, due to vaporization inside the cluster $x_e$, can be given as

$$q_c(t) = x_e \Gamma_G(t) L \qquad (8)$$

where $L$ denotes the latent heat of vaporization and $\Gamma_G(t)$ represents the rate of vapor mass generation per unit mixture volume. It is noteworthy that the homogeneous nucleation boiling i.e. boiling occurs without any cavity or surface effect has been not considered. With the assumption that all bubbles generated in different stage of liquid heating grow up independently, the rate, $\Gamma_G(t)$, can be calculated from the number of generated vapor bubbles and their growth according to the following integration:

$$\Gamma_G(t) = \int_0^t 4\pi r^2 \frac{\partial r(t,t')}{\partial t} \rho_v \quad J(T_l(t'))dt' \qquad (9)$$

For the number of bubbles, Carey [24] proposed the rate of homogeneous nucleation events per unit volume in a superheated liquid at temperature, $T_l$ as

$$J(T_l) = 1.44\times10^{40} \sqrt{\frac{\rho_l^2 \sigma}{M^3}} \exp \quad \frac{1.213\times10^{24}\sigma^3}{T_l\{P_s(T_l) \quad P_0\}^2} \qquad (10)$$

Blander and Katz [22] and Kagan [53] also derived the similar expressions for $J$. Figure 4 shows the variation of the nucleation event rate, $J$, with liquid temperature, $T_l$, for water at atmospheric pressure. The trend of variation of $J$ with $T_l$ is similar in all cases i.e. there is a very narrow temperature range below which homogeneous nucleation rate does not occur while above which it occurs instantaneously.

Next, for the bubble growth, Skripov [25] proposed as:

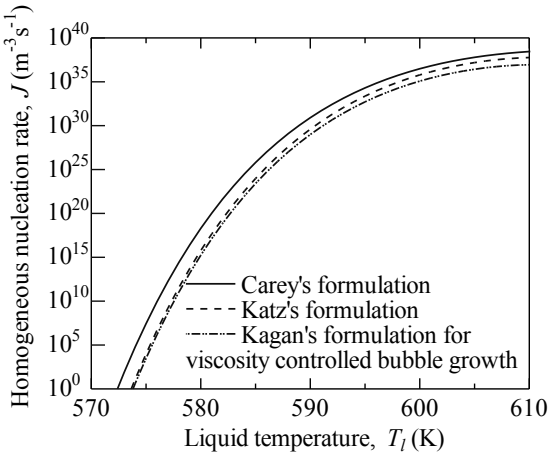


Fig 4. Radius of critical vapor embryo ($r_c$) at various liquid temperatures for water at atmospheric pressure.

$$r(t,t') = \phi\sqrt{t \quad t'} \qquad (11.a)$$

$$\phi = 2\sqrt{\frac{3}{\pi}} \frac{\sqrt{\lambda_l \rho_l c_l}}{L\rho_v} (T_l \quad T_s) \qquad (11.b)$$

where, $r(t, t')$ denotes the radius of a bubble at any time, $t$, which has been created at a time, $t'$.

Upon substituting Eq. (11) in Eq. (9) and substituting $T_l$ for $T_{avg}$, the expression of the instantaneous vapor generation rate per unit mixture volume, $\Gamma_G(t)$, can be obtained as a function of the average liquid temperature, $T_{avg}$, as follows

$$\Gamma_G(t) = 2\pi \int_0^t J(T_{avg}) \phi^3(T_{avg}) \rho_v \sqrt{t \quad t'} dt' \qquad (12)$$

Although $J$, $\phi$ and $\rho_v$ in Eq. (12) depend on the average liquid temperature, $T_{avg}$, the dependence of the nucleation rate, $J$, on $T_{avg}$ is particularly important due to the existence of $\sigma$ and $P_s$ in the exponential term. As some terms weakly depend on the liquid temperature, all terms other than the nucleation rate are taken out of the integral for simplicity. Finally, the following equation has been obtained for the instantaneous rate of boiling heat consumption due to homogeneous nucleation boiling, $q_c(t)$:

$$q_c(t) = 2\pi L \phi^3(T_{avg}) \rho_v x_e \int_0^t J(T_{avg}) \sqrt{t \quad t'} dt' \qquad (13)$$

By incorporating the expressions of $q_d(t)$ and $q_c(t)$ in Eq. (6), the following intrego-differential equation can be finally obtained for the average liquid temperature, $T_{avg}$, over the cluster of a characteristic size, $x_e$, with the consideration of simultaneous homogeneous nucleation boiling during non-equilibrium liquid heating.

$$\frac{dT_{avg}}{dt} = \frac{1}{\rho_l c_l x_e} \quad \lambda_l \left.\frac{\partial T}{\partial x}\right|_{x=0} \quad \left.\frac{\partial T}{\partial x}\right|_{x=x_e} \quad 2\pi L \phi^3 \left(T_{avg}\right) \rho_v x_e \int_0^t J\left(T_{avg}\right) \sqrt{t \quad t'}\, dt' \tag{14}$$

The initial condition for Eq. (14) corresponds to $T_{avg} = T_0$ at $t = 0$. The given governing equation i.e. Eq. (14) together with Eq. (5) (for $x_e = 2r_c$ with $T_l$ being replaced by $T_{avg}$) are complete enough for the closed form solution, if the temperature distribution in the liquid is given.

### 2.1 Procedure of Calculation

At first, any arbitrary thickness of the liquid control volume for instance, $x_{ei}$ is assumed with the average temperature, $T_{avg} = T_0$ at $t = 0$. For this arbitrarily chosen liquid control volume thickness, $x_{ei}$, the temporal variation of the average liquid temperature, $T_{avg}$, is then obtained by calculating the instantaneous energy deposition rate, $q_d(t)$ and energy consumption rate due to boiling, $q_c(t)$ in the liquid control volume as per Eq. (7) and Eq. (8). Note that the average temperature in the liquid volume may increase ($dT_{avg}/dt > 0$) or decrease ($dT_{avg}/dt < 0$) depending on the relative magnitude of instantaneous energy deposition rate, $q_d(t)$ and energy consumption rate $q_c(t)$ in the liquid cluster. How the average temperature will be varied with the liquid temperature will be shown later for various liquid heating conditions. At the beginning of the liquid heating process when the liquid temperature is not high enough for homogeneous nucleation to take place, external energy added to the liquid cluster, $q_d(t)$, causes only sensible heating ($q_c(t) = 0$ and $dT_{avg}/dt > 0$).

However, once homogeneous boiling initiates, $q_c(t)$ increases exponentially with the liquid temperature because the homogeneous nucleation rate, $J$, increases exponentially with the liquid temperature as shown in Fig.4. This tremendous increase in the energy consumption rate, $q_c(t)$, in the cluster, which in turn slows down the temperature rise in the liquid cluster and eventually a stage is reached at $t = t^*$, ($dT_{avg}/dt = 0$) at which $q_c(t)$ becomes equal to $q_d(t)$ with the maximum attainable liquid temperature in the cluster, $T_{avg} = T^*_{avg}$. This particular stage of bubble generation and growth has been defined as the boiling explosion in the present model after which further bubble nucleation and growth immediately causes the liquid sensible energy to decrease ($q_c(t) > q_d(t)$ and $dT_{avg}/dt < 0$). The maximum attainable temperature in the cluster, $T^*_{avg}$, obtained for $x_{ei}$ is then used to calculate the size of the critical vapor embryo, $2r_c$ ($T^*_{avg}$), as per Eq. (5) which is considered as the liquid control volume thickness or cluster size, $x_e$, for the next iteration. This iteration procedure is repeated until it converges, that is, the absolute value of $(x_e - x_{ei})/x_{ei}$ becomes less than 0.0001. Finally, the temperature rise in the liquid cluster is obtained for the cluster thickness, $x_e$, and the boiling explosion characteristics such as the liquid temperature limit ($T^*_{avg}$), the time ($t^*$) at the boiling explosion ($q_c(t) = q_d(t)$ and $dT_{avg}/dt = 0$) are determined.

## 3. APPLICATION OF NEW MODEL TO SPECIFIED CONDITION

In order to calculate the change of the average temperature given by Eq. (14) from a complete set of Eqs. (5) to (13), one first has to choose a specified boundary condition related to the boiling explosion phenomenon, which has been generally encountered during a rapid rise in liquid temperature by a direct heating of liquid and by a contact of liquid with high temperature solid as mentioned before. Therefore, we may apply this model to three different liquid heating cases namely, (1) liquid heating with linearly increasing temperature, (2) liquid heating at high heat flux pulse heating and (3) a contact of liquid with high temperature solid. Note that the initial and boundary conditions of liquid heating cases under consideration are identical to some of earlier experimental works reported in the literature.

### 3.1 Solutions for Three Different Conditions

The governing equation for heat conduction in the semi-infinite stagnant liquid becomes as

$$\frac{\partial T}{\partial t} = a \frac{\partial^2 T}{\partial x^2} \qquad \text{for } 0 < x \tag{15}$$

with a uniform temperature distribution of $T = T_0$ at $t = 0$. Provided that the boundary condition is given, then Eq. (15) can be solved. The solutions can be summarizes depending on the three different boundary conditions as given in the Table 1.

The solutions for the different boundary conditions are applied to predict the homogeneous nucleation boiling phenomena by combining them with from Eqs. (5) to (13).

### 3.2 Linearly Increasing Temperature

There are four different heating rates for water heating at atmospheric pressure, which had been considered with the identical initial boundary conditions reported by Gold et al. [28], Iida et al. [30], and Okuyama et al. [31]. The rate of temperature increase ranges from b = $37.3\times10^6$ K/s to $1.80\times10^9$ K/s [29, 30] using an initial liquid temperature of 293.15 K and Gold et al. [28] using an initial liquid temperature of 298.15 K. As one of examples, we choose the case [30] of $b = 37.3 \times 10^6$ K/s and then calculate the temporal variation of average liquid temperature, $T_{avg}$, along with the transient rates of external heat deposition, $q_d(t)$, and boiling heat consumption, $q_c(t)$, within the cluster which are shown in

Table 1: Boundary Conditions and Solutions [54]

| (1) Linearly increasing temperature | (2) High heat flux pulse heating | (3)Contact with high temperature solid |
|---|---|---|
| $T_w(t) = bt$ | $q_W = q$ | $T_i = \frac{\beta T_b + T_0}{1+\beta}$ and $\beta = \sqrt{\frac{(\rho c\lambda)_s}{(\rho c\lambda)_l}}$ |
| $T(x,t) = T_0 + 4bti^2\mathrm{erfc}\left(x/\sqrt{4\alpha t}\right)$ (16) | $T(x,t) = T_0 + \frac{q\sqrt{4\alpha t}}{\lambda} i\mathrm{erfc}(x/\sqrt{4\alpha t})$ (17) | $T(x,t) = T_0 + (T_i \quad T_0)\mathrm{erfc}\left(x/\sqrt{4\alpha t}\right)$ (18) |

figure 5.

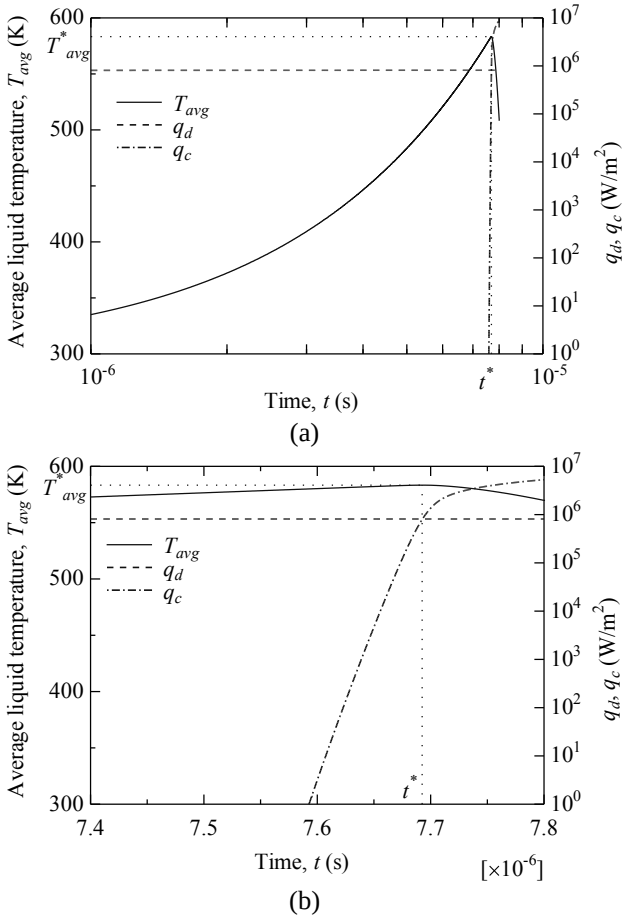


Fig 5. Temporal variation of average liquid temperature, external energy deposition rate and boiling heat consumption rate within the liquid control volume ($b$ = 37.3×10$^6$ K/s and $T_0$ = 298.15 K)

Figure 5(a) indicates that the deposited energy causes only sensible heating of the liquid during most of the heating process. No boiling heat consumption occurs until the liquid temperature reaches to a certain value because homogeneous nucleation occurs only when the liquid temperature reaches a certain temperature as shown in figure 4. Once boiling is initiated, the rate of boiling heat consumption increases sharply as the rate of homogeneous nucleation increases exponentially with liquid temperature. Upon closer observation on figure 5(b), which depicts the boiling phenomena on a magnified time scale, the rate of homogeneous boiling heat consumption in the cluster increases by over six orders of magnitude within approximately 0.10 μs after the commencement of homogeneous nucleation boiling. Increased boiling heat consumption at higher liquid temperature in turn slows the rate of liquid temperature escalation. As a result of these two mutually dependent processes, the liquid temperature ultimately reaches its maximum value, $T^*_{avg}$, when the rate of boiling heat consumption, $q_c(t)$, becomes equal to the rate of external energy deposition rate, $q_d(t)$, at $t = t^*$. After time, $t^*$, external energy deposition, $q_d(t)$, is no longer sufficient to support associated bubble generation and growth. In this situation, the huge number of bubble generations and these growth are accompanied by a corresponding decrease in the liquid sensible energy, which results in an autonomous evaporation condition as indicated in Fig. 5 by the sudden drop in the average liquid temperature curve after $t = t^*$. In addition, at this stage, vapor generation is assumed to be enough to occur on a massive scale that corresponds to possible boiling explosion or vapor explosion. In the present model, the criteria of boiling explosion has been defined as the onset of the loss of liquid sensible energy for the generation and growth of bubbles associated with the liquid boiling phenomena. More simply, boiling explosion is assumed to occur at time, $t = t^*$, with the maximum attainable liquid temperature, $T = T^*_{avg}$, under the following inequality of homogeneous boiling energy consumption and external energy deposition:

$$q_c(t) \geqslant q_d(t)$$

Figure 6 illustrates the time-temperature history for other heating rate of b = 37.3×10$^6$ K/s to 1.80×10$^9$ K/s. As shown in figure 6, with higher heating rates, the attainment of the boiling explosion condition is obtained much earlier while maximum attainable liquid temperature slightly is increased by raised be about 3 K within the change of b = 37.3×10$^6$ K/s to 1.80×10$^9$ K/s. The time at which boiling explosion takes place, proportionally decreases with an increase in the heating rate. Note that the term used in the model to describe the limit of maximum attainable liquid temperature ($T^*_{avg}$) is also common in slightly different forms in the literature, e.g., limit of maximum liquid superheat or limiting superheat temperature.

For the case of pulse heating experiments, Skripov [25] recommended the threshold nucleation rate to be in the range of $J$ = 10$^{18}$ to 10$^{28}$ m$^{-3}$s$^{-1}$. The iterative solution of the homogeneous nucleation rate equation for the maxima of this range of threshold nucleation rate yields a limiting liquid superheat temperature of 587 K. As shown in Fig. 7, the limit of maximum attainable liquid temperature has been found to be within the range of 583–587 K, depending on the heating rate ($b$) that ranges from 37.3×10$^6$ K/s to 1.80×10$^9$ K/s. Note that, the nucleation rate at the time of boiling explosion as per the model prediction, corresponds to approximately 10$^{23}$ to 10$^{28}$ m$^{-3}$s$^{-1}$, depending on the heating rate, $b$.

Figure 8 depicts the boiling configurations over a small film heater at different times as observed by Iida et al. [30], during rapid water heating from an initial liquid temperature of 298.15 K at a heating rate of 37.3×10$^6$ K/s at atmospheric pressure. As shown in Fig. 8, the condition of boiling explosion may be assumed to be between 7.65 μs and 7.85 μs when the entire heater surface is on the verge of being covered by a vapor blanket. In this case, the developed model predicts that the condition of boiling explosion will occur at 7.69 μs at

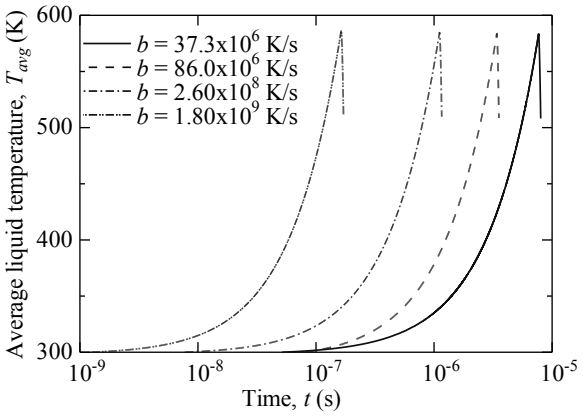


Fig 6. Temperature escalation during rapid water heating for various boundary heating rates ($b$)

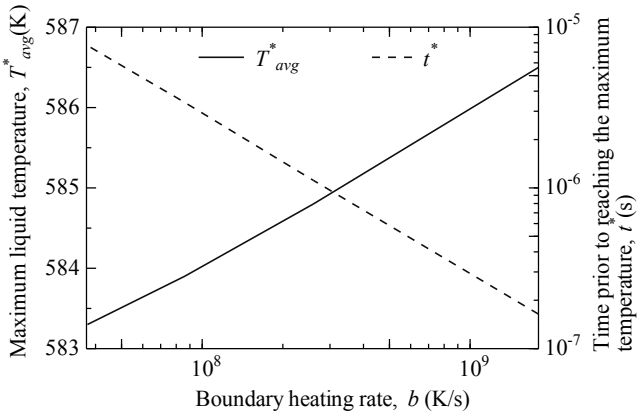


Fig 7. Effect of boundary heating rate ($b$) on maximum attainable liquid temperature ($T^*_{avg}$) and time prior to reaching the limit, i.e., boiling explosion ($t^*$)

Table 2: Summary of simulation results

| $T_0$ (K) | $b$ (K/s) | $T^*_{avg}$ (K) | $t^*$ (μs) | $x_e$ (nm) |
|---|---|---|---|---|
| 298.15 | 37.3×10$^6$ | 583.3 | 7.692 | 5.21 |
| 293.15 | 86.0×10$^6$ | 583.9 | 3.407 | 5.11 |
| 298.15 | 2.60×10$^8$ | 584.8 | 1.114 | 4.97 |
| 298.15 | 1.80×10$^9$ | 586.5 | 0.163 | 4.71 |

a maximum liquid temperature of 583.3 K. Figure 9 also presents the other photographs of progressive stages of explosive vaporization of water on an ultrathin Pt wire as reported by Gold et al. [28] for a heating rate of b = 86.0×10$^7$ K/s. As shown in the photographs, the wire surface is almost instantaneously covered by a thin vapor film. However, during the initial stages of vaporization, Gold et al. [28] pointed out "ready centers" on the wire surface that initiate and develop the boiling explosion process. As shown in Fig. 9, no significant change in the liquid pattern is observed until 3 μs after the start of heating. At 3.5 μs, the liquid is found to be driven away explosively from the wire surface due to possible bubble generation and growth as observed in Fig. 9(b). The thin vapor film over the wire surface at $t$ = 4.0 μs as shown in Fig. 9(c) is in fact due to the coalescence of numerous bubbles. For the identical initial and boundary conditions of Gold et al. [28], the model predicts that the boiling

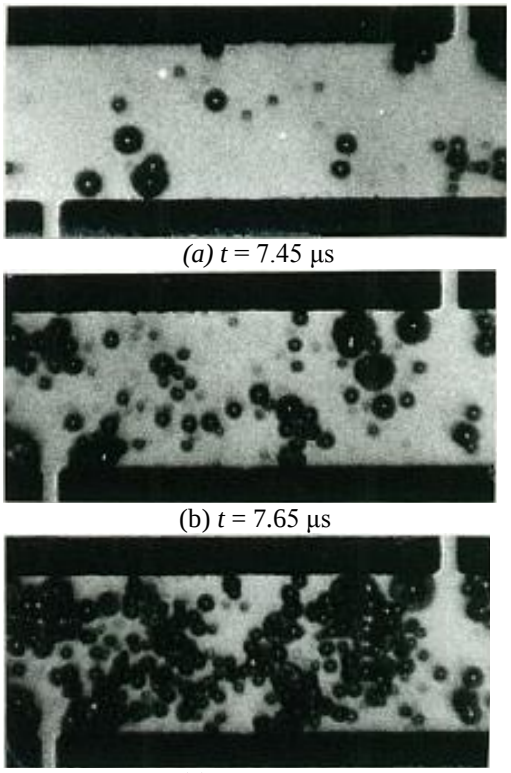

*(a)* $t$ = 7.45 μs

(b) $t$ = 7.65 μs

(c) $t$ = 7.85 μs

Fig 8. Boiling configurations over a small film heater at $b$ = 37.3×10$^6$ K/s and $T_0$ = 298.15 K [30]; Model predicted time of boiling explosion, $t^*$ = 7.692 μs

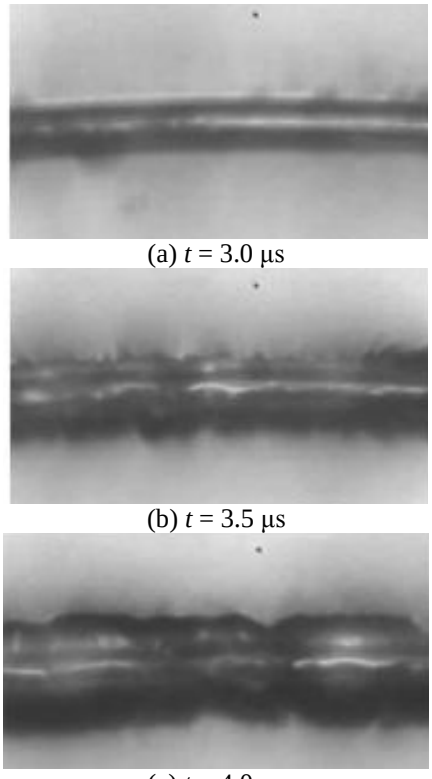

(a) $t$ = 3.0 μs

(b) $t$ = 3.5 μs

(c) $t$ = 4.0 μs

Fig 9. Progressive stages of explosive boiling at $b$ = 86.0 ×10$^6$ K/s and $T_0$ = 293.15 K [28]; Model predicted time of boiling explosion, $t^*$ = 3.407 μs

explosion condition to occur at 3.40 μs at a maximum liquid temperature of 583.9 K.

It may be worth mentioning that even higher heating rates of $2.60\times10^8$ K/s and $1.80\times10^9$ K/s [31], the observed time during which massive tiny bubbles appear, almost corresponds to the predicted time of 1.11 and 0.163 μs, which are in agreement within acceptable range, respectively. In addition to this, the corresponding maximum temperatures become 584.8 K and 586.5 K respectively.

### 3.3 High Heat Flux Pulse Heating

Recent advancement in MEMS technology has enabled the fabrication of planar film heaters in micron or even submicron scale that resulted in applicability of much high heat flux from the heater surface. Using the microfabrication technology, a polysilicon microheater can be fabricated with its surface totally free from noticeable cavities. Many experimental studies have been conducted by several research groups to understand the explosive boiling on microheaters immersed in liquids under the action of high heat flux pulse heating [34–40]. The solution for this case was already listed in Table 1.

Figure 10 depicts the temporal variation of the average cluster temperature, $T_{avg}$, along with the external energy deposition ($q_c$) and the energy consumption due to bubble nucleation and growth ($q_d$) in a characteristic liquid cluster during water heating with a heat flux, $q$ = 100 MW/m$^2$ from an initial liquid temperature, $T_0$ = 293 K. The size of the liquid cluster under consideration, $x_e$ = 5.39 nm. As shown in figures 10 (a) and 10 (b) the increasing energy consumption in the cluster at certain higher temperature range eventually leads to a situation under which energy consumption due to bubble nucleation and growth surpasses the external energy deposition in the cluster that causes the cluster sensible energy to decrease, which is the condition of the boiling explosion as defined in this model. For the liquid heating condition under consideration, the boiling explosion takes place at $t^*$ = 16.54 μs at the maximum cluster temperature, $T^*_{avg}$ = 582.25 K.

It is noteworthy that for the same heat flux, $q$ = 100 MW/m$^2$, and liquid initial temperature, $T_0$ = 298 K, the model predicts the boiling explosion to be at $t^*$ = 15.98 μs at the maximum cluster temperature, $T^*_{avg}$ = 582.26 K while the model proposed by Asai [35] corresponds the boiling explosion to be at a time of about 19.5 μs. Moreover, Asai [35] mentioned the homogeneous nucleation to occur within 5 nm of the heating surface to the ink liquid under the typical operating condition of bubble jet printer ($q$ = 100 MW/m$^2$) which is almost the same with the liquid cluster size considered in the present model. Figure 11 illustrates the progressive stages of boiling explosion in water observed during pulse heating experiments with $q$ = 265 MW/m$^2$ and $T_0$ = 293 K conducted by Hong et al. [39] together with the predicted time, $t^*$ = 2.39 μs. For this case, the maximum cluster temperature is predicted to be $T^*_{avg}$ = 583.6 K. On comparing the predicted time with the time of 2.1 μs at which the first bubble was observed, it was noticed that at $t$ = 3.0 μs, a massive vapor is observed on the heater and the predicted time is significantly earlier than the time of 3.0 μs. This time difference might be due to small amount of heat being dissipated into the back side of the heater during the heating process. As depicted in Fig. 11, the model prediction concerning the boiling explosion is found to be good consistent with experiments. It should be mentioned that the similar agreement can be obtained for other heat fluxes of $q$ = 253 MW/m$^2$ and 453 MW/m$^2$for which the predicted times become $t^*$ = 2.64 μs and $t^*$ = 0.98 μs, rspectively.

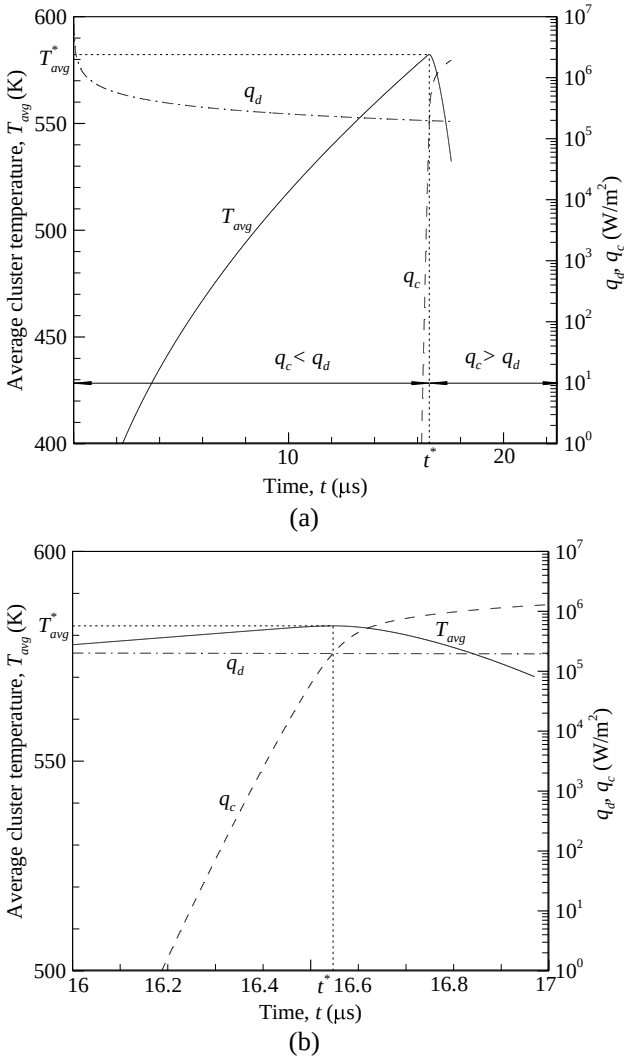


Fig 10. Temporal variation of temperature, external energy deposition and boiling heat consumption in the characteristic liquid luster ($q$ = 100 MW/m$^2$, $T_0$ = 293 K, $x_e$ = 5.39 nm)

Figure 12 shows the temperature rise inside the cluster during water heating with various heat fluxes, $q$, from a liquid initial temperature, $T_0$ = 293 K. As depicted in Fig. 12, the occurrence of the boiling explosion takes place much earlier at higher heat fluxes. The minimum heat flux necessary for the occurrence of the boiling explosion is important from some practical points of view. Note that, in the present model a characteristic time period of 1 millisecond for the occurrence of the boiling explosion to determine the limiting heat flux for boiling explosion.

Beyond this characteristic time period, heterogeneous nucleation might play the key role for boiling incipience. As shown in Fig. 12, for the liquid initial temperature of 293 K, the value of the minimum heat flux for water corresponds to about 15 MW/m$^2$.

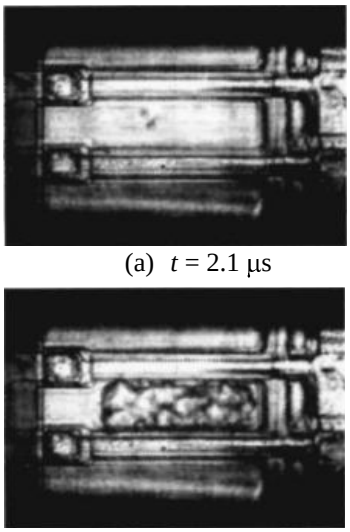

(a) $t$ = 2.1 μs



(b)$t$ = 3.0 μs

Fig 11. Experimental observation of boiling explosion in water at ($q$ = 265 MW/m$^2$, $T_0$ = 293 K) [38]; model predicted time for boiling explosion: $t^*$ = 2.39 μs

Asai [35] also mentioned the minimum heat flux or the threshold heat flux to be in order of 100 MW/m$^2$ for reproducible and powerful bubble generation processes. As mentioned in Ref. [35], the nucleation process becomes more random for heat fluxes lower than the threshold limit. This randomness in the nucleation process might be due to the heterogeneous nucleation which might take place after 1 millisecond from the commencement of heating process as considered in the present model. The apparent difference between the limiting heat fluxes for boiling explosion reported in Refs. [35] and as obtained in the present model might be due to various unexpected factors involved in the experimentations. However, this difference might be considered acceptable from engineering point of view. Zhao et al. [55] have also mentioned the criteria for minimum heat flux for explosive boiling to occur on the basis of maximum possible heat flux across the liquid-vapor interface, $q_{max,.max}$. For water at atmospheric pressure, they speculated a minimum heat flux of 224 MW/m$^2$ to be required for explosive boiling.

As shown in figure 12, the time of the boiling explosion strongly depends on the heat flux, $q$. For the liquid initial temperature, $T_0$ = 293 K, a variation of about two orders in the magnitude of the heat flux, $q$, (15–1000 MW/m$^2$) has been found to result in a variation of about three orders in the magnitude of the boiling explosion time, $t^*$, (0.723 ms–0.173 μs). However, for a particular heat flux, the time of the occurrence of the boiling explosion also depends on the liquid initial temperature as the nucleation occurs earlier for a higher liquid initial temperature. A similar trend of the variation of the boiling explosion time, $t^*$, with heat flux, $q$, has been obtained for the liquid initial temperatures, $T_0$, ranging from 293 K to 373 K. In the present study, the following

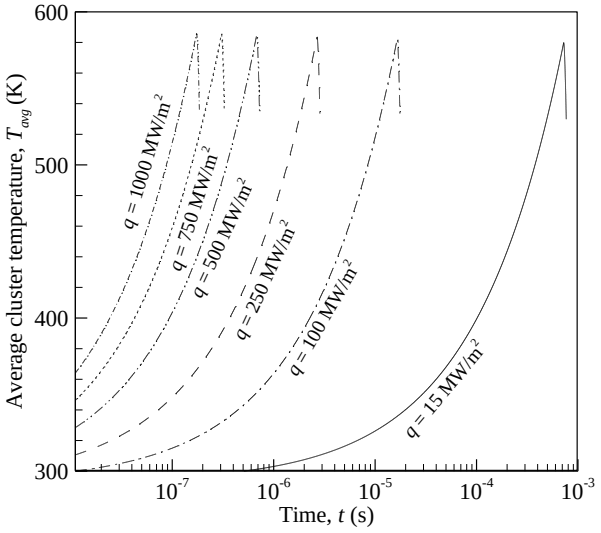


Fig 12. Temperature rise inside a characteristic liquid cluster for various heat fluxes ($T_0$ = 293 K)

approximate Eq. (19) has been proposed for the time of the boiling explosion, $t^*$ (μs), for water heating at atmospheric pressure as a function of the heat flux, $q$ (MW/m$^2$) and liquid initial temperature, $T_0$ (K) as

$$t^* = [1.71 \quad 0.01(T_0 \quad 273)] \times 10^5 q^{\,1.98} \qquad (19)$$

for 15 < $q$ < 1000 MW/m$^2$ and 293 < $T_0$ < 373 K.

Unlikely to the time of the boiling explosion $t^*$, the maximum cluster temperature, $T^*_{avg}$, that is the liquid temperature at the boiling explosion did not change much with the variation in the heat flux. However, the liquid penetrates deeper in the metastable region prior to the boiling explosion during heating with higher heat fluxes. In the present study, for a variation of the heat flux, $q$, from 15 MW/ m$^2$ to 1000 MW/m$^2$, the maximum attainable cluster temperature, $T^*_{avg}$, has been found to increases about 6K only (580–586 K). However, no substantial effect of the liquid initial temperature, $T_0$, on the maximum attainable liquid temperature, $T^*_{avg}$, has been found, for example; $T^*_{avg}$ changes only about 0.2 K as $T_0$ varies from 293 K to 373 K with $q$ = 100 MW/m$^2$. This fact might be due to the occurrence of the nucleation phenomena at much higher temperature range (~575 K) than the liquid initial temperatures (293–373 K). Therefore, the variation of the maximum attainable liquid temperature, $T^*_{avg}$ (K) at the boiling explosion has been expressed as a function of the heat flux, $q$ (MW/m$^2$) only as Eq. (20).

$$T^*_{avg} = 1.43\ln(q) + 575.9 \qquad (20)$$

for 15 < $q$ < 1000 MW/m$^2$

Note that the temperature limit at the boiling explosion obtained in the present study for water at atmospheric pressure has been found to be in good agreement with the limiting superheating temperature obtained by Varlamov et al. [38] for pulse heating conditions (587 K).

### 3.4 Contact with High Temperature Solid

Liquid interaction in contact with preheated solid

surface is everyday occurrence that comprises a great variety of thermo-fluid mechanical facets such as the deposition of a single or multiple drops, spray cooling, jet impingement quenching, fire extinguishing. In these applications, boiling explosion due to homogeneous nucleation occurs in some situations depending on the pre-contact temperatures of the solid and the liquid and also their thermo-physical properties. For more clarification, we refer herein the experimental observation made by Woodfield et al. [8] during jet impingement quenching as shown in Fig. 13. Figure 13 shows a typical cooling curve and recorded audible sound obtained by Woodfield et al. [8] during jet impingement quenching. As the authors [8] explained, the first strong sound could be heard as a sharp spattering sound and a repetition of wet and dry surface conditions takes place at very short period. Note that the wet surface condition mentioned here refers to the surface condition during direct solid-liquid contact while dry surface condition refers to that after boiling explosion that might occur due to rapid liquid heating during brief solid-liquid contact. It is interesting that during the repetition of wet and dry surface conditions, the measured thermocouple does not show any change because a short period change in surface temperature does not penetrate to the thermocouple sensor location.

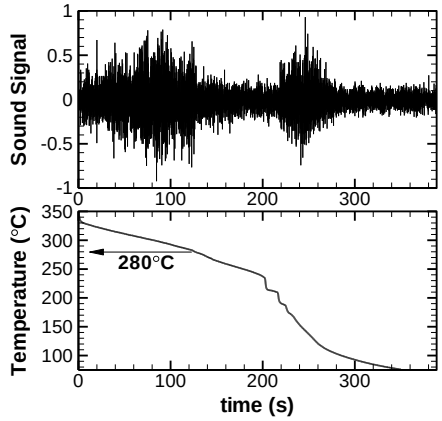


Fig 13. Audible sound during quench (embedded thermocouple reading: 4 mm from center and 5 mm beneath the surface; Mat.: Cu, $T_b$= 350 °C; Water jet: $u_j$ = 3 m/s, $T_0$ = 49 °C) [8]

On closer observation at the early stages of jet impingement quenching, Islam et al. [9] found a chronological change in liquid flow patterns over the surface depending on the surface temperature and then pointed out that a chaotic flow pattern occurs when the surface temperature remains above a certain limit, $T_{limit}$, while a calm sheet like flow pattern appears as the surface cools down below $T_{limit}$. Note that the limiting surface temperature, $T_{limit}$, has been defined by the authors with the presumption of jet impingement on a solid surface as a two semi-infinite body contact problem with a constant thermodynamic superheat limit of the liquid, $T_{TSL}$ (as assumed to be 312°C for water at atmospheric pressure). The analytical expression of $T_{limit}$, the precontact liquid jet temperature ($T_0$), the limit of maximum liquid superheat ($T_{TSL}$) and the thermo-physical properties of the solid block and the liquid jet can be given as follows as mentioned in [53]:

$$\frac{T_{limit} - T_{TSL}}{T_{TSL} - T_0} = \frac{1}{\beta} = \sqrt{\frac{(\rho c \lambda)_l}{(\rho c \lambda)_s}} \qquad (21)$$

Islam et al. [9] speculated from a many of observed flow patterns, that unstable film boiling or explosive boiling might be the possible heat transfer mode in the early stages of jet impingement quenching; some brief solid-liquid contact makes the surface wet and cool while the subsequent boiling explosion makes the surface again dry during which surface temperature recovers due to heat conduction inside the solid. With the repetition of wet and dry surface condition, the surface ultimately cools down below a certain limit ($T_{limit}$) that allows stable solid liquid contact without any boiling explosion. To apply the present model of homogeneous nucleation boiling explosion to the case of liquid heating that occurs during brief solid-liquid contact, the heat transfer process has been considered as a two semi-infinite solid contact problem. With this assumption, the solution for this case can be obtained as given by Eq. (18) in Table1.

Figure 14 shows numerical result during contact of a water jet ($T_0$ = 20 °C) with a hot steel surface ($T_b$ = 350 °C) and the graphical definition of the boiling explosion condition ($q_c(t) > q_d(t)$), at which the average temperature rise ($T_{avg}$) inside a characteristic liquid cluster ($x_e$ = 5.17 nm) starts to decrease ($dT_{avg}/dt < 0$) with an impending autonomous large scale vapor generation.

Figure 15 depicts the temporal variation of the average cluster temperature, $T_{avg}$, along with the external energy deposition ($q_c$) and the energy consumption due to bubble nucleation and growth ($q_d$) in the cluster during water heating when a water jet (20 °C) comes in contact with hot steel surface at various temperatures (335–550 °C). As shown in Fig 15, in the case of liquid contact with higher temperature surface, the liquid is heated up to a much higher temperature prior to the attainment of the boiling explosion condition and also the time necessary to attain the boiling explosion condition, $t^*$, decreases sharply. Note interestingly that for the special case of surface temperature, $T_b$ = 335°C; the liquid temperature asymptotically approaches the interface temperature without attainment of the boiling explosion condition. This phenomenon points it out that for solid temperatures at or below 335°C with all other quench condition being same, the vapor generation during direct solid-liquid contact is not high enough to hinder stable solid-liquid contact. In other words, flow patterns corresponding to the surface temperature at or below 335 °C would be calm and quiet as stable solid-liquid contact is established in these conditions. For solid surfaces, at a temperature higher than 335 °C, boiling explosion in the cluster will result in unstable repetition of wet and dry surface condition and therefore chaotic flow patterns until its temperature is cooled down below 335 °C in a fashion similar to that obtained by Woodfield et al. [8] as shown in figure 16.

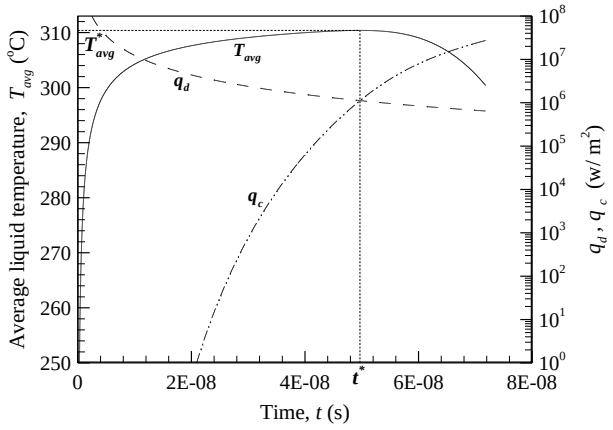


Fig 14. Temporal variation of average liquid temperature, external energy deposition and homogeneous nucleate boiling energy consumption in a liquid cluster ($T_b$ = 350 °C, $T_0$ = 20 °C, $x_e$ = 5.17 nm)

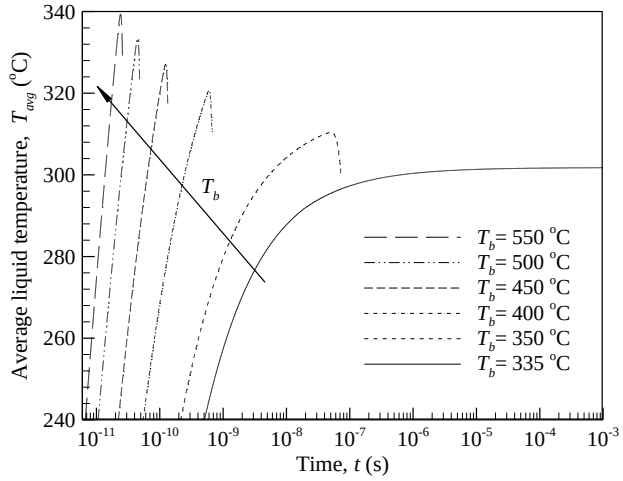


Fig 15. Average liquid temperature escalation inside the liquid cluster during contact of a water jet (20 °C) with steel surface at various temperatures (335–550 °C)

Moreover, Woodfield et al. [8] reported the calm and quiet flow condition with steady solid-liquid contact to occur at a surface temperature of 280 °C as shown in Fig. 13. Results predicted by the present model differ from that of Woodfield et al. [8] due to the variation of quench conditions (solid-liquid combination and liquid initial temperature) between these two cases under consideration. However, the limiting condition of steady solid-liquid contact in both cases can be compared in terms of the corresponding interface temperature, $T_i$. According to the present model, there is no boiling explosion due to homogeneous nucleation boiling at a solid surface temperature of 335 °C with a corresponding interface temperature of 303 °C. The interface temperature for the Woodfield et al. experiment [8] becomes 337 °C at the moment of the first liquid contact with the solid. After repetitions of solid-liquid contact, the surface temperature goes down to 280 °C at which the interface temperature assumes a value of about 270 °C. Considering 303 °C as the limiting interface boundary temperature for the occurrence of the boiling explosion due to homogeneous nucleation only, the observed explosive liquid flow pattern and the recorded high pitch sound in Woodfield's experiment [8] might be due to homogeneous nucleation boiling for the surface temperatures ranging from 350 °C to 314 °C (corresponding to the interface temperature 303°C for the given solid-liquid combination and their pre-contact temperatures) while that might be due to heterogeneous nucleation boiling for the surface temperatures ranging from 314 °C to 280 °C.

The effect of solid surface temperature on the characteristics of homogeneous nucleation boiling explosion phenomena has been manifested in Table 3. As mentioned in Table 3, the limit of maximum attainable liquid temperature increases over 30 °C for an increase of 200 °C in the solid surface temperature while the time of boiling explosion decreases about two orders of magnitude for the same variation. The size of the liquid cluster under consideration also decreases with the increase in the solid surface temperature.

Table 3: Homogeneous nucleation characteristics during quench of carbon steel surface (350–500°C) with water jet (20°C) at atmospheric pressure

| $T_0$ (°C) | $T_b$ (°C) | $T_i$ (°C) | $x_e$ (nm) | $T^*_{avg}$ (°C) | $t^*$ (ns) |
|---|---|---|---|---|---|
| 20 | 350 | 316.5 | 5.17 | 310.4 | 49.68 |
| | 400 | 361.4 | 3.71 | 320.5 | 0.595 |
| | 450 | 406.3 | 2.96 | 327.1 | 0.123 |
| | 500 | 451.3 | 2.41 | 333.4 | 0.044 |
| | 550 | 496.2 | 2.40 | 339.3 | 0.024 |

Regarding the limit of maximum attainable liquid temperature, it is interesting that the present model ascertains a relatively higher value of the maximum attainable liquid temperature as compared to other values reported in the literature. For instance, the limit of maximum attainable liquid temperature is found to be reported about 303°C [28] for water at atmospheric pressure. This variation is due to the fact that the limit of maximum liquid superheat during liquid heating depends on the rate of liquid heating itself [28].

Eberhart [16] mentioned, the liquid spinodal temperature or the thermodynamic superheat limit of a liquid based on thermodynamic and mechanical stability consideration exceeds the kinetic superheat limit determined by droplet-heating or pulse heating technique or predicted by homogeneous nucleation theory. Up to present, the maximum liquid heating rate applied during pulse heating experiments in water corresponds to about $10^9$ K/s [31]. However, during contact with very hot surfaces, the liquid might undergo heating at a rate several order higher than pulse heating experiments. Therefore, it is more likely that during liquid contact with sufficiently preheated surface, the liquid might be heated to the maximum possible limit of superheat i.e. the thermodynamic superheat limit. From a survey of many experimental evidences of the superheat limit for water, Eberhart and Pinks [56], concluded that the limit of superheat for water at atmospheric pressure might be 329 ± 3°C. The energy based approach of Salla et al. [57] also results in a thermodynamic limit of liquid superheat 333.2 °C for water at atmospheric pressure.

## 4. LOWER LIMIT OF HOMOGENEOUS NUCLEATION BOILING EXPLOSION IN WATER

The limiting condition for boiling explosion due to homogeneous nucleation is very important for better design and control of various thermal micromachines based on the principle of explosive boiling. This is also important for the prediction of the onset of stable wetting during liquid contact with hot surfaces as in case of jet impingement quenching or spray quenching. In order to determine the lower limit for the occurrence of homogeneous nucleation boiling explosion for water at atmospheric pressure, the present model has been adopted as described in section 2 with two different boundary conditions, namely, linearly increasing temperature condition and constant temperature condition.

### 4.1 Liquid Heating with Linearly Increasing Temperature

This condition essentially describes the pulse heating technique and droplet superheat technique in the bubble column. These two techniques have been frequently applied to determine experimentally the liquid superheat limit. In the present study, the heating rate has been considered to vary from 10 K/s to $10^9$ K/s. The upper limit of this range includes the typical heating rate used in pulse heating experiments [28, 30, 31] while the lower limit corresponds to a typical droplet superheating condition [58]. Also the liquid initial temperature has been considered to vary from 0 °C to 100 °C. Figure 16 depicts the temperature rise inside the cluster and also the occurrence of homogeneous boiling explosion for various heating rates with the initial liquid temperature, $T_0$ = 20 °C. As shown in Fig. 16, the boiling explosion condition i.e. the onset of the decrease of average cluster temperature due to bubble nucleation and growth takes place earlier for higher heating rates. The summary of simulations has been presented in Table 4. As mentioned in Table 4, the size of cluster under the consideration gradually decreases for higher rates of heating. As mentioned in Table 4, for a variation of eight orders of magnitude in the heating rate the maximum attainable temperature at which homogenous boiling explosion occurs, increases about 11 °C only while the corresponding time of homogeneous boiling explosion changes roughly by eight orders of magnitude.

It is interesting that, the nucleation rates, $J$ ($m^{-3}s^{-1}$), at the boiling explosion for different heating rates as obtained in the present model study are of similar order of "threshold nucleation" rates for different liquid superheating techniques as mentioned in Ref. [23]. For instance, for typical droplet superheat experiment and pulse heating experiment, a nucleation rate of $J = 10^{12} – 10^{13}$ $m^{-3}s^{-1}$ and $J = 10^{24} – 10^{29}$ $m^{-3}s^{-1}$ respectively is considered as the threshold nucleation rate [23]. However, the nucleation rate at the boiling explosion as per the present model corresponds to a value of $J = 10^7$ $m^{-3}s^{-1}$ and $J = 10^{26}$ $m^{-3}s^{-1}$ for a representative droplet superheating experiment ($b$ = 10 K/s) and pulse heating experiment ($b$ = $10^9$ K/s) respectively. For better understanding, one might be interested in the number of bubbles generated in the cluster prior to the boiling explosion, $J$ ($1/m^2$), has been considered as

$$J^* = x_e \int_0^{t^*} J(t)dt \qquad (22)$$

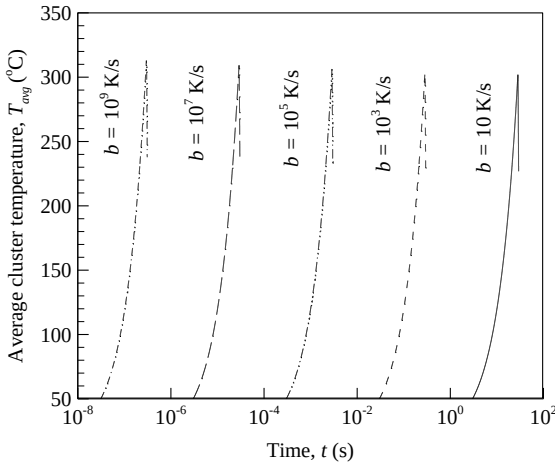


Fig 16. Temperature escalation inside a characteristic liquid cluster for various heating rates ($T_0$ = 20 °C)

As mentioned in Table 4, $J^*$, increases sharply with the heating rate. For the case of $b$ = 10 K/s, $J^*$ is obtained to be less than unity. This is due to the fact that the cluster in the liquid can appear in any location as the temperature in the liquid is raised almost uniformly. Therefore, one should consider larger liquid volume in place of $x_e$ in which boiling explosion might occur. As the characteristics of the liquid temperature field during liquid heating with a linearly increasing temperature depend only on the rate of temperature rise. Therefore, liquid initial temperature, $T_0$, has no effect on the cluster temperature at the boiling explosion. At any particular rate of heating higher liquid initial temperature results in earlier occurrence of the boiling explosion at a constant maximum attainable cluster temperature which depends only on the heating rate

Table 4: Homogeneous nucleation boiling at various heating rates ($b$)

| $T_0$ (°C) | $b$ (K/s) | $x_e$ (nm) | $T^*_{avg}$ (°C) | $t^*$ (s) | $J^*$ ($1/m^2$) |
|---|---|---|---|---|---|
| 20 | 10 | 6.72 | 301.8 | $2.82\times10^{1}$ | 0.007 |
| | $10^3$ | 6.32 | 303.9 | $2.84\times10^{-1}$ | 6.17 |
| | $10^5$ | 5.88 | 306.3 | $2.87\times10^{-3}$ | $5.19\times10^{3}$ |
| | $10^7$ | 5.38 | 309.2 | $2.90\times10^{-5}$ | $4.20\times10^{6}$ |
| | $10^9$ | 4.79 | 312.8 | $2.97\times10^{-7}$ | $3.07\times10^{9}$ |

### 4.2 Liquid Heating with Constant Temperature Condition

Liquid heating with constant temperature boundary condition occurs when a liquid comes in with a hot solid surface. The heat transfer process between the contacting solid and liquid can be assumed to be a two 1-D semi-infinite body contact problem liquid with a constant interface temperature, $T_i$, determined by the initial liquid temperature, the solid temperature and the

thermo-physical properties of the solid-liquid combination through a parameter as $\beta$ .

The temperature rise inside the cluster during water (20 °C) contact with hot steel surfaces (335–340 °C) at atmospheric pressure is shown in Fig. 17. As shown in Fig. 17, during contact with higher temperature surfaces, the condition of homogeneous nucleation boiling explosion appears much earlier with a relatively higher cluster temperature. For the case of liquid contact with the surface at 335 °C, the condition of homogeneous boiling explosion does not occur within a time period of 1 millisecond. After this characteristic time period, heterogeneous nucleation boiling might play the key role for vaporization. The summary of simulation results is listed in Table 5. From Table 5, it is evident that boiling explosion over hot steel surface occurs within a characteristic time period of about 1 millisecond, for a surface temperature at or above 336 °C for water contact with an initial water temperature of 20 °C at atmospheric pressure. This lower limiting condition of homogeneous boiling explosion corresponds to a maximum liquid temperature of about 303 °C at the boiling explosion with a limiting interface temperature of around 304 °C.

Note that the number of bubbles generated in the cluster prior to the boiling explosion, $J^*$, depends much on the surface temperature. During contact with lower temperature surface, slow and steady liquid heating might result in clusters/bubbles beyond the cluster thickness as in the case of extremely slow heating case ($b$ = 10 K/s) as discussed in Sec. 4.1.

As obtained in the present study, for a particular liquid initial temperature and particular solid-liquid combination, there exists a limiting surface temperature say, $T^*_b$, below which no homogeneous nucleation boiling explosion occurs. The variation of this limiting surface temperature with the liquid initial temperature has been tabulated in Table 6 for water contact with hot steel surface. Theoretically, the limiting interface temperature as well as the liquid temperature in the cluster at the boiling explosion should be the same for all combinations of $T_0$ and $T^*_b$. However, as a margin of 1 K has been allowed in defining the limiting surface temperature for homogeneous boiling explosion, some variations occurred in the corresponding limiting interface temperature as well as in the maximum attainable cluster temperature for different combinations of $T_0$ and $T^*_b$ as mentioned in Table 6. However, with an average interface temperature, $T^*_i$ = 304 °C for all combinations of $T_0$ and $T^*_b$, the condition of homogeneous boiling explosion has been found to occur around at a maximum attainable cluster temperature, $T^*_{avg}$ = 303°C, within a time period of about 0.5 millisecond after contact. Note that the temperature limit obtained for this case of liquid heating are close to the temperature limit at which homogeneous boiling explosion also occurs during slow and steady heating with a linearly increasing temperature condition ($b$ = 10 K/s). Moreover, this temperature limit at the homogeneous boiling explosion is the same as that predicted by Lienhard's [18] correlation for homogeneous nucleation in water at atmospheric pressure.

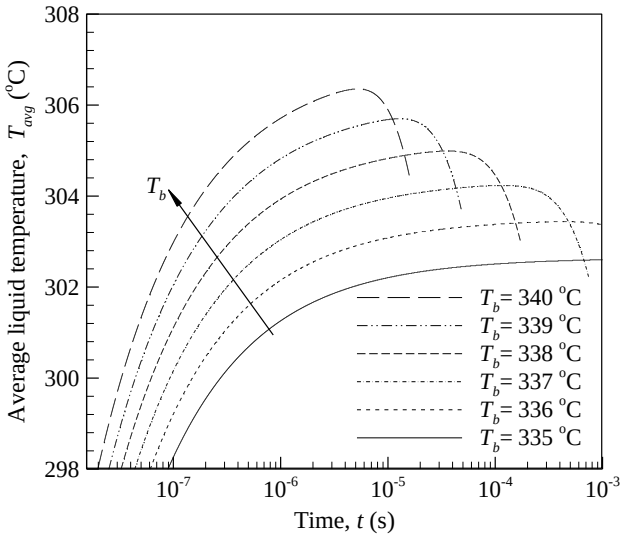


Fig 17. Temperature escalation inside a characteristic liquid cluster during water contact with hot steel surfaces ($\beta$ = 8.86, $T_0$ = 20 °C)

Table 5: Homogeneous nucleation boiling during liquid contact with hot steel surface at various temperatures ($\beta$ = 8.86, $T_0$ = 20 °C)

| $T_0$ (°C) | $T_b$ (°C) | $T_i$ (°C) | $x_e$ (nm) | $T^*_{avg}$ (°C) | $t^*$ (μs) | $J^*$(1/m$^2$) |
|---|---|---|---|---|---|---|
| 20 | 335 | 303.0 | 6.55 | - | - | - |
| | 336 | 303.9 | 6.41 | 303.4 | 443.46 | 0.48 |
| | 337 | 304.8 | 6.26 | 304.2 | 117.42 | 6.90 |
| | 338 | 305.7 | 6.12 | 305.0 | 36.11 | $7.36\times10^{1}$ |
| | 339 | 306.6 | 5.99 | 305.7 | 12.85 | $5.92\times10^{2}$ |
| | 340 | 307.5 | 5.87 | 306.3 | 5.239 | $3.67\times10^{3}$ |

Table 6: Limiting condition of homogeneous nucleation boiling over hot surface ($\beta$ = 8.86) during liquid contact at various temperatures (0–100 $^0$C)

| $T_0$ (°C) | $T^*_b$ (°C) | $T_i$ (°C) | $x_e$ (nm) | $T^*_{avg}$ (°C) | $t^*$ (s) |
|---|---|---|---|---|---|
| 0 | 338 | 303.7 | 6.45 | 303.2 | $5.3\times10^{-4}$ |
| 20 | 336 | 303.9 | 6.41 | 303.4 | |
| 40 | 334 | 304.2 | 6.36 | 303.6 | |
| 60 | 331 | 303.5 | 6.47 | 303.1 | |
| 80 | 329 | 303.7 | 6.42 | 303.3 | |
| 100 | 327 | 304.0 | 6.38 | 303.6 | |

The limiting surface temperature above which instantaneous homogeneous boiling explosion occurs might be discussed in terms of the Leidenfrost temperature which is commonly referred to as the minimum surface temperature at which stable film boiling exists. As mentioned in Table 6, the limiting surface temperature for steel surface might be in the range of 338–327 °C depending on the initial water temperature ranging from 0 °C to 100 °C. Godlesky and Bell [59] reported a temperature of 320 °C as the Leidenfrost temperature for water-steel combination. Gunnerson and Cronenberg [60] also speculated the theoretical limit of Leidenfrost temperature to be

100–363 °C for steel-water combination.

With the pre-assumption of the liquid-solid contact problem as two 1-D semi-infinite body contact problem, once the limiting interface temperature for homogeneous boiling explosion is known, it is possible to determine the limiting surface temperature for liquid contact with any other solid surfaces readily from the definition of the interface temperature as follows

$$T_b^* = T_i^* + \frac{1}{\beta}\left(T_i^* \quad T_0\right) \tag{23}$$

The variation of the limiting surface temperature, $T^*_b$, for homogeneous boiling explosion during water contact with steel ($\beta$ = 8.86), brass ($\beta$ = 11.06) and copper ($\beta$ = 22.63) has been tabulated in Table 7 and also shown in Fig. 19 for various liquid initial temperatures ranging from 0 °C to 100 °C for a limiting interface temperature of homogeneous boiling explosion, $T^*_i$ = 304 °C. The inter-dependency among $T^*_b$, $T_0$ and $\beta$ presents a boundary surface in a $T_b$–$T_0$–$\beta$ co-ordinate system as shown in Fig. 20 above which boiling explosion due to homogeneous nucleation occurs instantaneously and below which it does not.

Table 7: Limiting surface temperature for homogeneous nucleation boiling during water contact with various hot surfaces

| $T^*_i$ (°C) | $\beta$ | $T_0$ (°C) | $T^*_b$ (°C) |
|---|---|---|---|
| 304 | 8.86 | 0–100 | 338–327 |
| | 11.06 | | 331–322 |
| | 22.63 | | 317–313 |

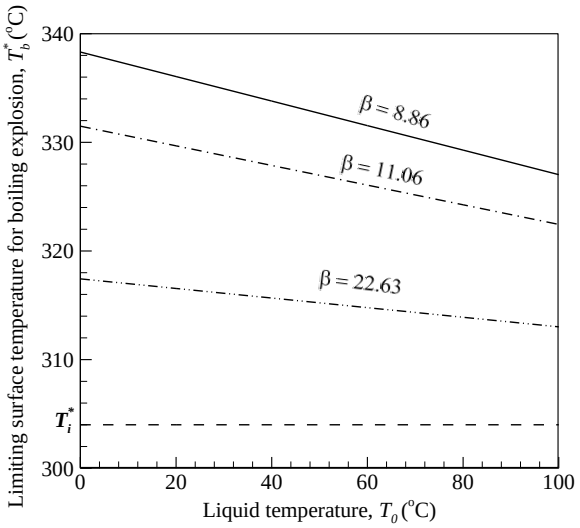


Fig 19. Limiting surface temperature ($T^*_b$) for homogeneous boiling explosion at various liquid initial temperatures ($T_0$)

## 5. COMPARISON BETWEEN ATTAINABLE MAXIMUM HEAT FLUX WITH UPPER BOUND OF MAXIMUM HEAT FLUX AND CONTINUUM CHARACTERISTICS

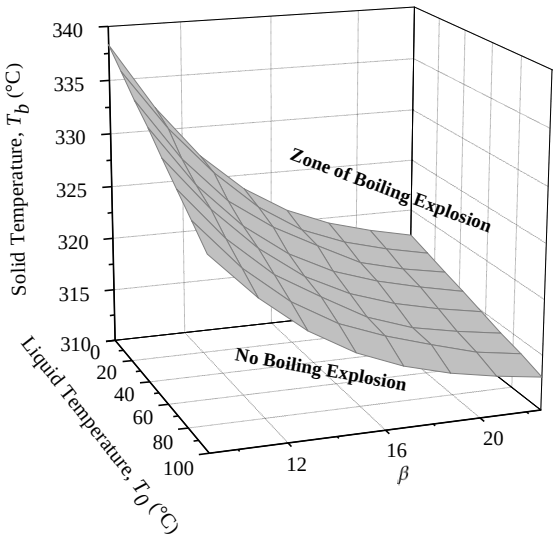


Fig 20. Boundary for homogeneous boiling explosion on $T_b - T_0 - \beta$ plane

The boiling explosion condition as defined in the present model might be compared with the theoretical explosion condition in terms of the maximum possible heat flux across the liquid-vapor interface, $q_{max,max}$. As proposed by Gambill and Lienhard [61], the maximum possible heat flux across the liquid-vapor interface, $q_{max,max}$, that can be conceivably achieved in a vaporization or condensation process can be expressed as follows

$$q_{max,max} = \rho_v L\sqrt{RT/2\pi} \tag{24}$$

The heat flux across the liquid-vapor interface of a bubble $q_{l\text{-}v}$, can be obtained as

$$q_{l\ v} = \rho_v L\frac{dr}{dt} \tag{25}$$

If $q^*_{l\text{-}v}$ corresponds to the heat flux across the liquid-vapor interface of a bubble at the time of boiling explosion, $t = t^*$, then

$$q^*_{l-v} = \rho_v L\frac{dr}{dt}\Big|_{t=t^*} \tag{26}$$

Bubbles of different sizes co-exist at $t = t^*$. Therefore, the individual bubble has its own growth rate depending on its life time that is the bubble grows at the different heat flux across the liquid-vapor interface. We choose the largest heat flux at the interface of the bubble which is generated just before the boiling explosion namely at the time $t = t^*$. Near the time, $t = t^*$, the growth of this bubble is essentially controlled by the inertia and to calculate the heat flux, $q^*_{l\text{-}v}$, with the consideration of inertia controlled bubble growth; we adopted the bubble growth model as proposed by Rayleigh as mentioned in Ref. [62].

### 5.1 Linearly Increasing Boundary Temperature

Table 8 summarizes the heat flux characteristics across

the liquid-vapor interface of bubble and also the number of molecules in the cluster at the boiling explosion for various linearly increasing temperature cases. As shown in Table 8, the largest heat flux, $q^*_{l\text{-}v}$, is lower than the maximum limit, $q_{max,max}$, for all values of heating rates considered herein. This is due to the fact that the limit of maximum possible heat flux, $q_{max,max}$, is obtained with the unique assumption of no condensation at the liquid-vapor interface. In reality, there must be some condensation in parallel with the vaporization during the bubble growth. It is important to clarify the length scale of the critical vapor embryo which has been taken as the size of cluster in the present model for the application of macroscopic property values, such as surface tension and density. As continuum characteristics, the number of molecules within a critical bubble at the time of boiling explosion has been considered. It has been found that the number of molecules within the vapor embryo at the time of boiling explosion exceeds 100 for all values of heating rates under consideration as mentioned in Table 8.

Table 8: Heat flux across the liquid-vapor interface, $q^*_{l\text{-}v}$, and $q_{max,max}$ and number of molecules inside the critical vapor embryo ($N$) at the boiling explosion ($t = t^*$) for various linearly increasing temperature case

| $T_0$ (K) | $b$ (K/s) | $q^*_{l\text{-}v}$ (W/m$^2$) | $q_{max,max}$ (W/m$^2$) | $N$ |
|---|---|---|---|---|
| 298.15 | $37.3\times10^6$ | $7.22\times10^9$ | $1.49\times10^{10}$ | 135 |
| 293.15 | $86.0\times10^6$ | $7.31\times10^9$ | $1.50\times10^{10}$ | 128 |
| 298.15 | $2.60\times10^8$ | $7.44\times10^9$ | $1.52\times10^{10}$ | 120 |
| 298.15 | $1.80\times10^9$ | $7.71\times10^9$ | $1.55\times10^{10}$ | 105 |

Incidentally, Henry and Fauske [41] mentioned that a minimum of 40 molecules to be required to produce vapor bubble and therefore a liquid layer containing about 40 molecules might be enough for the boiling explosion to take place. Hence, with the number of molecules in the vapor embryo exceeding 100, the continuum characteristics has been assumed to be satisfied, that is, this phenomenon can be still treated with from the macroscopic point of view.

Table 9: Heat flux across the vapor interface ($q^*_{l\text{-}v}$) and limit of maximum heat flux "$q_{max,max}$" at $t = t^*$ for water (20 °C) contact with hot steel surfaces (350-550 °C) at various temperatures and the number of molecules in the critical vapor embryo

| $T_b$ (°C) | $t^*$ (ns) | $q^*_{l\text{-}v}$ (W/m$^2$) | $q_{max,max}$ (W/m$^2$) | $N$ |
|---|---|---|---|---|
| 350 | 49.68 | $7.25\times10^9$ | $1.50\times10^{10}$ | 133 |
| 400 | 0.595 | $9.05\times10^9$ | $1.68\times10^{10}$ | 59 |
| 450 | 0.123 | $1.09\times10^{10}$ | $1.81\times10^{10}$ | 34 |
| 500 | 0.044 | $1.47\times10^{10}$ | $1.92\times10^{10}$ | 21 |
| 550 | 0.024 | $2.26\times10^{10}$ | $2.01\times10^{10}$ | 20 |

### 5.2 Constant Boundary Temperature

As mentioned in Table 9, the boiling explosion occurs from fractions of a nanosecond to few nanoseconds upon liquid contact with the surface depending on the surface temperature. Therefore, no visual observation of boiling explosion during jet impingement quenching can be made so far even though very fast video camera is used [9]. Under this condition, how much heat flux occurs at the liquid-vapor interface at the time of boiling explosion might be important to judge the corresponding boiling explosion condition. As mentioned in Table 9, the heat flux across the liquid-vapor interface at the time of boiling explosion, $q^*_{l\text{-}v}$, is lower than the maximum limit, $q_{max,max}$, for the contact with a lower temperature solid surface. However, for the cases with a higher temperature solid surface, $q^*_{l\text{-}v}$ ultimately approaches $q_{max,max}$. This variation of $q^*_{l\text{-}v}$ with the surface temperature simply points out that, during contact of a liquid with very hot surface, the boiling explosion occurs almost instantaneously resembling the hypothetical condition of "no return of vapor molecules" at the liquid-vapor interface as assumed by Gambill and Lienhard [61]. In addition, from Table 9, it may be noted that, at a solid block temperature beyond about 550 °C, the boiling explosion may occur at the heat flux, $q_{max,max}$, because $q^*_{l\text{-}v}$ never becomes larger than $q_{max,max}$. As mentioned in Sec. 5.1, the present model is based on the continuum condition and the number of molecules in the critical bubble at the boiling explosion has been considered as the continuum characteristic. As mentioned in Ref. [63], continuum consideration may be applicable for liquid thickness over 10 molecular layers. Therefore, with the presence of about 20 molecules in the critical bubble, it has been assumed that the continuum characteristic has been satisfied.

## 6. CONCLUSION

A new theoretical model to study the homogeneous boiling explosion phenomena during non-equilibrium heating have been developed in the present study. The main outcomes of the present research can be summarized as:

(1) A new theoretical model based on the idea of 1-D heat conduction and the theory of homogeneous nucleation boiling has been developed to study the boiling explosion phenomena.
(2) An appropriate size of liquid layer known as the characteristic liquid cluster has been proposed for non-equilibrium practical liquid heating conditions. Therefore, the present model has been generalized that is independent of liquid heating condition.
(3) While boiling explosion had been defined arbitrarily in earlier research, a particular stage of liquid heating has been defined as the boiling explosion in the present study that is the onset of decrease of liquid sensible energy due to massive scale vaporization.
(4) The condition of the boiling explosion defined in the present model has been found to be in good agreement with experimental microscale boiling explosion.
(5) The variation of liquid flow patterns observed in early stages of jet impingement quenching is due to the occurrence of homogeneous boiling explosion.
(6) In the case of jet impingement quenching, the time needed for the occurrence of boiling explosion depends strongly on the surface temperature and may

vary from fraction of a millisecond to that of a nanosecond.

(7) The longest time scale for the homogeneous boiling explosion to occur during jet impingement quenching or by any other liquid heating condition might be considered to be in the order of 1 millisecond.

(8) For water at atmospheric pressure, the temperature limit at the boiling explosion corresponds to a value of about 303 ℃ in any liquid heating condition.

(9) The limiting interface temperature for water contact with any hot surface as obtained in the present study corresponds to about 304 ℃. For the cases with solid-liquid temperature higher than 304 ℃, instantaneous boiling explosion will hinder direct solid-liquid contact. Therefore, no stable wetting is possible for water jet impingement as long as the surface temperature is cooled down enough to have solid-liquid temperature lower than 304 ℃.

(10) For linear heating of water, the heating rate should be higher than $10^6$ K/s for homogeneous boiling explosion while for water heating with high heat flux heating, this condition corresponds to a heat flux of $1.5\times10^6$ W/m$^2$.

## 6. ACKNOWLEDGEMENT

The present study was supported by a Grant-in-aid for Scientific Research (B) 20360101, 2008.

## 7. NOMENCLATURE

| | | |
|---|---|---|
| $a$ | Thermal diffusivity | m$^2$/s |
| $b$ | Rate of boundary temperature rise | K /s |
| $c$ | Specific heat | kJ/(kgK) |
| $J$ | Rate of homogeneous nucleation events | 1/( m$^3$s) |
| $J^*$ | Number of bubbles generated in the cluster ($x_e$) at $t = t^*$ | (1/m$^2$) |
| $M$ | Molecular weight | kg/(molK) |
| $P_o$ | Bulk liquid pressure | Pa |
| $P_s$ | Saturation pressure | Pa |
| $q$ | Boundary heat flux | W/m$^2$ |
| $q_{in}$ | Incoming heat flux to the cluster at $x = 0$ | W/m$^2$ |
| $q_{out}$ | Outgoing heat flux from the cluster at $x = x_e$ | W/m$^2$ |
| $q_d$ | Rate of energy deposition to the liquid cluster | W/m$^2$ |
| $q_c$ | Rate of boiling heat consumption in the liquid cluster | W/m$^2$ |
| $q_{l\text{-}v}$ | Heat flux across the liquid vapor interface | W/m$^2$ |
| $q^*_{l\text{-}v}$ | Heat flux across the liquid vapor interface at $t = t^*$ | W/m$^2$ |
| $q_{max,max}$ | Theoretical upper limit of evaporative heat flux across the liquid vapor interface | W/m$^2$ |
| $r$ | Bubble radius | m |
| $r_c$ | Radius of the critical vapor embryo | m |
| $R$ | Universal gas constant | J/(kgK) |
| $t$ | Time | S |
| $t'$ | Time of bubble generation | S |
| $t^*$ | Time of the boiling explosion | S |
| $T$ | Temperature | K or °C |
| $T_{avg}$ | Average temperature in the liquid cluster | K or °C |
| $T^*_{avg}$ | Maximum attainable cluster temperature | K or °C |
| $T_b$ | Solid surface temperature | °C |
| $T^*_b$ | Limiting surface temperature for homogeneous boiling explosion | °C |
| $T_i$ | Interface temperature | °C |
| $T^*_i$ | Limiting interface temperature for homogeneous boiling explosion | °C |
| $T_0$ | Liquid initial temperature | K or °C |
| $x$ | Distance from the boundary | M |
| $x_e$ | Size of the liquid cluster ($2r_c$) | M |
| ***Greek*** | | |
| $\lambda$ | Thermal conductivity | W/(mK) |
| $\sigma$ | Surface tension | N/m |
| $\rho$ | Density | kg/m$^3$ |
| $\Gamma$ | Rate of vapor generation per unit mixture volume | kg/(m$^3$s) |
| ***Subscripts*** | | |
| $l$ | Liquid | |
| $s$ | Solid | |
| $v$ | Vapor | |

## 8. REFERENCES

1. P. E. Schick, T. M. Grace, Review of smelt-water explosions, Institute of Paper Chemistry: Appleton, Wisconsin Project No. 3473–2, 1982
2. R. C. Reid, Superheated liquids, Amer. Sci. 64: 146, 1976
3. P. D. Hess, K. J. Brondyke, Molten aluminum-water explosions, Met. Prog. 95: 93, 1969.
4. R. C. Reid, Rapid phase transitions from liquid to vapor, Adv. Chem. Eng. Vol. 12 pp. 105–207, 1983.
5. D. S. Burgess, J. N. Murphy, and M. G. Zabetakis, Hazards associated with the spillage of liquefied natural gas on water, U.S Bureau of Mines Rep. Invest. No. 7448, 1970.
6. D. S. Burgess, J. Biordi, and J. Murphy, Hazards of spillage of LNG into water, U.S Bureau of Mines, PMSRC Rep. No. 4177, 1972.
7. A. W. Cronenberg, Recent developments in the understanding of energetic molten fuel coolant interactions, *Nucl. Safety* Vol. 21, pp. 19–337, 1980.
8. P. L. Woodfield, M. Monde, and A. K. Mozumder, Observation of High Temperature Impinging-jet Phenomena, *International Journal of Heat and*

*Mass Transfer* Vol. 48, pp. 2032–2041, 2005.
9. M. A. Islam, M. Monde, P. L. Woodfield, and Y. Mitsutake, Jet Impingement Quenching Phenomena for Hot Surfaces well above the Limiting Temperature for Solid-Liquid Contact, *International Journal of Heat and Mass Transfer* Vol. 51, pp. 1226–1237, 2008.
10. A. Asai, Application of the nucleation theory to the design of bubble jet printers, *Jpn. J. Applied Physics*, Vol. 28, pp. 909-915, 1989.
11. M. Gad-el-Hak, The MEMS handbook, CRC Press, Boca Raton, 2002.
12. M. Staples, K. Daniel, M. J. Cima, R. Langer, Application of micro and nano-electromechanical devices to drug delivery, *Pharma. Res.* Vol. 23, PP. 847–863, 2006.
13. D. J. Laser, J. G. Santiago, A Review of Micropumps, *J. Micromech. Microeng*. Vol. 14, R35–R64, 2004.
14. Y. K. Lee, U. C. Yi, F. G. Tseng, C. J. Kim, C. M. Ho, Fuel injection by a thermal microinjector, Proceedings of MEMS, ASME International Mechanical Engineering, Nashville, Tennessee, USA, pp 419–425, 1999.
15. D. K. Maurya, S. Das, S. K. Lahiri, Silicon MEMS vaporizing liquid microthruster with internal microheater, J. Micromech. Microeng. Vol. 15, pp. 966–970, 2005.
16. J. G. Eberhart, The Thermodynamic and the Kinetic Limits of Superheat of a Liquid, Journal of Colloid and Interface Science, Vol. 56(2) pp. 262–269, 1976.
17. P. Spiegler, J. Hopenfeld. M. Silberberg, C. F. Bumpus Jr., and A. Norman, Onset of Stable Film Boiling and the Foam Limit, *International Journal of Heat and Mass Transfer* Vol. 6, pp. 987–994, 1963
18. J. H. Lienhard, Corresponding States Correlations of the Spinodal and Homogeneous Nucleation Limits, *Journal of Heat Transfer*, Vol. 104, pp. 379–381, 1984.
19. S. G. Kandilikar, M. Shoji, V. K. Dhir, Handbook of Phase Change: Boiling and Condensation, Taylor & Francis, U.S.A.
20. M. Volmer, and A. Webber, Keimbildung in ubersattigten Gebilden, *Z. Phys. Chem.*, Vol. 119, pp. 277–301, 1926.
21. W. Doring, Die Uberhitzungsgrenzeund Zerreibfestigkeitvon Flussigkeiten, *Z. Phys. Chem.*, Vol. 36, pp. 371–386, 1937.
22. M. Blander, and J. L. Katz, Bubble Nucleation in Liquids, *AIChE Journal*, Vol. 21(5), pp. 833–848, 1975.
23. R. Cole, Boiling Nucleation, Advances in Heat Transfer, Academic Press, Vol. 10, pp. 86–166, 1974.
24. V. P. Carey, Liquid-Vapor Phase Change Phenomena, Hemisphere Publishing Corporation, 1994
25. V. P. Skripov, Metastable Liquids, Wiley, New York, 1974
26. V. P. Skripov, and P. A. Pavlov, Explosive Boiling of Liquids and Fluctuation Nucleus Formation, *High Temperature (USSR)*, Vol. 8, pp. 782–787, 833–839, 1970.
27. K. P. Derewnicki, Experimental Studies of Heat Transfer and Vapor Formation in Fast Transient Boiling, *International Journal of Heat and Mass Transfer* Vol. 28, pp. 2085–2092, 1985.
28. S. Gold, D. Poulikakos, Z. Zhao, and G. Yadigaroglu, An investigation of microscale explosive vaporization of water on an ultrathin Pt wire, *International Journal of Heat and Mass Transfer*, Vol. 45, pp. 367–379, 2002.
29. Y. Iida, K. Okuyama, and K. Sakurai, Peculiar bubble generation on a film heater submerged in ethyl alcohol and imposed a high heating rate over $10^7$ K/s, *International Journal Heat and Mass Transfer*, Vol. 36 (10), pp. 2699–2701, 1993.
30. Y. Iida, K. Okuyama, and K. Sakurai, Boiling Nucleation on a very small film heater subjected to extremely rapid heating, *International Journal Heat and Mass Transfer*, Vol. 37 (17), pp. 2771–2780, 1994.
31. K. Okuyama, S. Mori, K. Sawa, and Y. Iida, Dynamics of boiling succeeding spontaneous nucleation on a rapidly heated small surface, *International Journal Heat and Mass Transfer*, Vol. 49, pp. 2771–2780, 2006.
32. C. T. Avedisian, W. S. Osborne, F. D. McLeod, and C. M. Curly, Measuring Bubble Nucleation Temperature on the Surface of a Rapidly Heated Thermal Ink-Jet Heater Immersed in a Pool of Water, Proceedings of Royal Society, London, A 445, pp. 3875–3899.
33. V. V. Kuznetsov, and I. A. Kozulin, Explosive Vaporization of a Water Layer on a flat Microheater, *Journal of Engineering Thermophysics*, Vol. 19 (2), pp. 102–109, 2010.
34. A. Asai, T. Hara, and I. Endo, One Dimensional Model of Bubble Growth and Liquid Flow in Bubble Jet Printers, *Japanese Journal of Applied Physics*, Vol. 26 (10), pp. 1794–1801, 1987.
35. A. Asai, Application of the Nucleation Theory to the Design of Bubble Jet Printer, *Japanese Journal of Applied Physics*, Vol. 28 (5), pp. 909–915, 1989.
36. A. Asai, Bubble dynamics in boiling under high heat flux pulse heating, *ASME Journal of Heat Transfer*, Vol. 113, pp. 973–979, 1991.
37. Z. Yin, A. Prosperetti, and J. Kim, Bubble Growth on an Impulsively Powered Microheater, *International Journal Heat and Mass Transfer*, Vol. 47, pp. 1053–1067, 2004.
38. Yu. D. Varlamov, Yu. P. Meshcheryakov, M. P. Predtechenskii, S. I. Lezhnin and S. N. Ulýankin, Specific Features of Explosive Boiling of Liquids on a Film Microheater, *Journal of applied Mechanics and technical physics*, Vol. 48 (2), pp. 213–220, 2007.
39. Y. Hong, N. Ashgriz, and J, Andrews, Experimental Study of Bubble Dynamics on a Micro Heater Induced by Pulse Heating, *ASME Journal of Heat Transfer*, Vol. 126, pp. 259–271, 2004.

40. J. Xu, and W. Zhang, Effect of Pulse Heating Parameters on the Microscale Bubble Dynamics at a Microheater Surface, *International Journal Heat and Mass Transfer*, Vol. 51, pp. 389–396, 2008.
41. R. D. Henry, and H. K. Fauske, Nucleation Process in Large Scale Vapor Explosions, *ASME Journal of Heat Transfer*, Vol. 101, pp. 280–287, 1979.
42. M. Ochiai, and S. G. Bankoff, A Local Propagation Theory for Vapor Explosion, Paper No. SNI 6/3, in the Proceedings of Third Special Meeting on Sodium/Fuel Interactions in Fast Reactors, Tokyo, Japan, 1976.
43. Y. Iida, T. Takashima, T. Watanabe, H. Ohura, C. Ogiso and N. Araki, A Fundamental Study of Thermal Interaction of Molten Salt and Cold Liquid, in the Proceedings of 19th National Heat Transfer Symposium of Japan, Nagoya, pp. 511–513, 1982.
44. I. Ueno and M. Shoji, Thermal-Fluid Phenomena Induced by Nanosecond-Pulse Heating of Materials in Water, *ASME Journal of Heat Transfer*, Vol. 123, pp. 1123–1133, 2001.
45. X. Huai, Z. Dong, D. Liu, and G. Wang, An Experimental Study of Microscopic Explosive Boiling Induced by Pulsed-Laser Irradiation, Proceedings of ASME International Mechanical Engineering Congress, Vol. 3, pp. 205–212, 2002.
46. X. Huai, Z. Dong, D. Liu, Z. Dong, R. Jin, and G. Wang, Rapid Transient Explosive Boiling of binary Mixture under Pulsed-Laser Irradiation, *Science in China (Series E)*, Vol. 46 (5), pp. 490–496, 2003.
47. Yu. E. Geints, A. A. Zemlyanov, and R. L. Armstrong, Explosive Boiling of water droplets irradiated with intense $Co_2$-laser radiation: Numerical Experiments, *Applied Optics*, Vol. 33 (24), pp. 5805–5810, 1994
48. F. S. Gunnerson, and A. W. Cronenberg, A Thermodynamic Prediction of the Temperature for Film Boiling Destabilization and its Relation to Vapor Explosion Phenomena, ANS Annual meeting, Sandiego, USA, 1978.
49. V. Gerweck and G. Yadigaroglu, A local Equation of State for Fluid in the Presence of a wall and Its Application to Rewetting, *International Journal Heat and Mass Transfer*, Vol. 35, pp. 1823–1832, 1992.
50. S. Inada, and W. J. Yang, Mechanism of Miniaturization of Sessile Drops on a Heated Surface, *International Journal Heat and Mass Transfer*, Vol. 36, pp. 1505–1515, 1993.
51. E. Elias, P. L. Chambre, Liquid Superheat during Nonequilibrium Boiling, *Heat Mass Transfer*, Vol. 45, pp. 659–662, 2009.
52. M. N. Hasan, M. Monde, and Y. Mitsutake, Model for Boiling Explosion during Rapid Liquid Heating, *International Journal Heat and Mass Transfer*, Vol. 54, pp. 2844–2853, 2011.
53. Yu. Kagan, The Kinetics of Boiling of a Pure Liquid, *Russian Journal of Physical Chemistry*, Vol. 34:42, 1960.
54. H. S. Carslaw, J. C. Jaeger, Conduction of heat in Solids, 2nd Edition, Oxford University Press, New York 1959.
55. Z. Zhao, S. Gold, and D. Poulikakos, Pressure and power generation during explosive vaporization on a thin-film micorheater, *International Journal Heat and Mass Transfer*, Vol. 43, pp. 281–296, 2000.
56. J. G. Eberhart, and V. Pinks, The Thermodynamic Limit of Superheat of Water, *Journal of Colloid and Interface Science*, Vol. 7(2) 1985.
57. J. M. Salla, M. Demichela, and J. Casal, BLEVE: A New Approach to the Superheat Limit Temperature, *Journal of Loss and Prevention in the Process Industries*, Vol. 19, pp. 690–700, 2006.
58. P. G. Debenedetti, , Metastable Liquids: Concepts and Principles, Princeton University Press, 1996
59. E. S. Godlesky and K. J. Bell, Proceedings of 3rd International Heat Conf. Vol. 4, p. 51 AIChE, N.Y., 1966.
60. F. S. Gunnerson, and A. W. Cronenberg, A Thermodynamic Prediction of the Temperature for Film Boiling Destabilization and its Relation to Vapor Explosion Phenomena, ANS Annual meeting, Sandiego, USA, 1978.
61. W. R. Gambill, J. H. Lienhard, An upper bound for the critical boiling heat flux, ASME Journal of Heat Transfer, Vol. 111, pp. 815–818, 1989.
62. N. I. Kolev, Multiphase Flow Dynamics, 3rd Edition, Vol. 2, Springer, Berlin, 2007.
63. M. Gad-el-Hak, The Fluid Mechanics of Microdevices- the Freeman Scholar Lecture, *Journal of Fluid Engineering*, Vol. 121, pp 690–700, 1999.

## 9. MAILING ADDRESS

**Masanori Monde**
Department of Mechanical Engineering,
Saga University, Japan
**E-mail:** monde@me.saga-u.ac.jp